Cytoneme-mediated intercellular signaling in keratinocytes is essential for epidermal remodeling in zebrafish

Yi Wang[1], Thomas Nguyen[1], Qingan He[1], Oliver Has[1], Kiarash Forouzesh[1], Dae Seok Eom[1,2,3*]

[1]Department of Developmental and Cell Biology, University of California, Irvine, CA 92617, USA
[2]Center for Complex Biological Systems, University of California, Irvine, CA 92697, USA
[3]UC Irvine Skin Biology Resource Center, University of California, Irvine, CA 92697, USA

Summary

The skin, the largest organ, functions as a primary defense mechanism. Epidermal stem cells supply undifferentiated keratinocytes that differentiate as they migrate toward the outermost skin layer. Although such a replenishment process is disrupted in various human skin diseases, its underlying mechanisms remain elusive. With high-resolution live imaging and in vivo manipulations, we revealed that Notch signaling between keratinocytes is mediated by signaling filopodia called cytonemes and is essential for proper keratinocyte differentiation and proliferation. Inhibiting keratinocyte cytonemes reduced Notch expression within undifferentiated keratinocytes, leading to abnormal differentiation and hyperproliferation, resembling human skin disease phenotypes. Overproduction of Interleukin (IL)-17 signal, associated with skin diseases like *psoriasis*, induces psoriatic phenotypes by reducing cytoneme extension in zebrafish. Our study suggests that intercellular signaling between keratinocytes through cytonemes is critical for epidermal maintenance, and its misregulation could be an origin of human skin diseases.

Introduction

The vertebrate skin is a multilayered structure comprised of three main layers: the epidermis, the dermis, and the hypodermis [1]. Each layer has distinct anatomical characteristics and serves specific functions. Of these layers, the epidermis, as the outermost layer, plays a pivotal role as the body's first line of defense against environmental threats such as pathogens. It also plays a crucial role in regulating body temperature and preventing water loss into the surrounding environment. The epidermis consists of various layers, including the stratum basale, which houses a single layer of stem cells, and several layers of differentiated cells, including the stratum spinosum, stratum granulosum, and stratum lucidum. The outermost layer, the stratum corneum, primarily comprises dead keratinocytes that are continuously shed and replenished by underlying cells differentiated from epidermal stem cells in mammals [3].

In zebrafish, the epidermis shares a similar composition to that of mammals. However, unlike mammals, aquatic animals lack a cornified layer and instead rely on a mucous layer to protect the epidermis in the aquatic environment. The basal layer of zebrafish, equivalent to the mammalian stratum basale, consists of stem cells that provide keratinocytes for replenishment during epidermal remodeling or wound healing. The periderm, comparable to the mammalian stratum granulosum and lucidum, is where fully differentiated keratinocytes are found. Similar to mammalian stratum granulosum,

an intermediate layer is present between the basal layer and the periderm, housing undifferentiated keratinocytes [2]. This intermediate layer is formed during metamorphosis and persists throughout adulthood in zebrafish [4].
The maintenance of a healthy epidermal barrier requires on the intricately controlled proliferation and differentiation of keratinocytes, which are supplied from underlying basal stem cells [5]. As keratinocytes migrate apically from the stem cell layer, they undergo differentiation while concurrently exhibit proliferation within the intermediate layer. Ultimately, fully differentiated keratinocytes replenish the periderm. This replenishment mechanism is well-conserved in both zebrafish and humans, and its mis-regulation constitutes a pivotal factor in the etiology of various human skin diseases, including *psoriasis*, *atopic dermatitis*, and others [2,6-9]. Studies have also revealed that maintaining a healthy epidermis requires complex intercellular communications between keratinocytes and the immune system, adding complexity to our efforts to comprehensively understand the mechanism behind this process [5,10].
One of the major signaling pathways critical for keratinocyte differentiation and proliferation is the Notch pathway. Studies have demonstrated that Notch receptors and ligands exhibit spatially restricted expression patterns in the layers of the epidermis [7]. Notch 1, 2, and 3 are notably prevalent in the undifferentiated keratinocytes in mice [11-13]. Moreover, dysregulated Notch signaling has been linked to abnormal keratinocyte differentiation and hyperproliferation, which are one of the hallmarks of various skin diseases including *psoriasis* and *atopic dermatitis* [14], highlighting the importance of proper Notch signaling in epidermal maintenance to retain the balance between keratinocyte differentiation and proliferation [15,16]. Nonetheless, the precise mechanisms underlying the initiation of Notch signaling in undifferentiated keratinocytes and its dynamic regulations are not yet understood.
Furthermore, various combinations of cytokines produced by different immune cells under inflammatory conditions can significantly contribute to the onset or progression of these skin diseases. Among these, interleukin-17 (IL-17) is a well-characterized cytokine closely associated with the symptoms of these conditions. The overproduction of IL-17 by T helper (Th)17 cells and other immune cells is a primary driver of certain skin diseases, such as *psoriasis*. Biologic treatments that inhibit IL-17 have proven to effectively alleviating the symptoms of these conditions [17]. Unfortunately, discontinuing these treatments often lead to symptom recurrence. Also known side effects associated with these inhibitors include headaches, nasopharyngitis, and infections [18]. Consequently, a definitive cure remains elusive currently [6,19].
Thus, IL-17 is one of the key molecules that contribute to the development of *psoriasis* and other skin diseases. The IL-17 pathway exerts its effects on keratinocytes, endothelial cells, and immune cells resulting in the production of additional cytokines that promote positive feedback loops, sustaining the inflammatory state [17]. However, the underlying cellular and molecular mechanisms of this process are not yet fully understood. Therefore, gaining a comprehensive understanding of the interplay between keratinocytes, the Notch pathway, IL-17, and other players is essential for advancing the treatment of these diseases.

Intercellular signaling plays a critical role in skin development and maintenance. In recent years, a growing body of evidence has demonstrated that cells can establish

communication through long, thin cellular protrusions extended by cells involved in either sending or receiving signals. These protrusions can be categorized based on their cytoskeletal composition, mode of signal delivery, morphology, and other characteristics. Examples include cytonemes, airinemes, tunneling nanotubes, intercellular bridges, migrasomes, exophers, and more [20-24]. These specialized cellular protrusions have been observed in diverse cell types and species, ranging from fruit flies and sea urchins to zebrafish and mice, with their signaling roles experimentally confirmed *in vivo* [20,24-27]. These specialized protrusions are significantly longer than typical filopodia and establish direct contact with target cells and serve as highways for transporting signaling molecules for major signaling pathways such as Hedgehog, Wnt, TGFβ, FGF, Notch in many *in vivo* and *in vitro* contexts [25]. These signaling cellular protrusions temporally exist and have thin actin or actin/tubulin-based filaments. Consequently, live imaging is considered one of the most effective methods for observing these structure. For that reason, zebrafish has emerged as an excellent model system for studying these cellular protrusions. The transparent nature of their early developing embryos makes zebrafish particularly well-suited for this purpose. Moreover, zebrafish are vertebrates that share common mechanisms with mammals in terms of epidermal remodeling and maintenance [28-30].

In this study, we show evidence that cytonemes extended by fully differentiated keratinocytes play a crucial role in activating Notch signaling in undifferentiated keratinocytes, thus contributing to the maintenance of epidermal homeostasis and remodeling in zebrafish. Furthermore, we demonstrate that IL-17, a key player in the pathogenesis of human skin diseases, and *clint1*, a gene required for epidermal homeostasis, regulate keratinocyte cytonemes [31,32]. Collectively, our findings shed light on the mechanisms that govern the regulation of skin replenishment through keratinocyte cytonemes, providing a novel perspective on understanding how skin diseases can originate from keratinocytes autonomously through the mediation of cellular protrusions.

Results

Differentiated keratinocytes extend cytoneme-like cellular protrusions

In previous studies, we have reported a unique type of signaling cellular protrusions known as 'airinemes' and have investigated their signaling roles in pigment cells of zebrafish [20,33-36]. To extend our understanding of airinemes in other cell types, we employed random cell labelling and identified several cell types that extend airineme-like protrusions featured by highly curved filaments and large vesicles at their tips [4,20,34]. Fully differentiated keratinocytes, marked by *krt4*, were among the cell types displaying these airineme-like protrusions [4] (Figure 1A, arrowhead). These keratinocytes intriguingly also extend cytoneme-like protrusions, characterized by relatively straight filaments and a lack of vesicle at the tips [20,21,24] (Figure 1A-B, arrowheads). Nevertheless, we observed a low incidence of airineme-like protrusions, contrasting with the more frequent occurrence of cytoneme-like structures in these keratinocytes (Figure 1C). Consequently, we conducted a more in-depth characterization of these cytoneme-like protrusions. It is noted that cytonemes primarily consist of actin filaments, whereas airinemes are both actin and tubulin-based structures [20]. To affirm their nature, we utilized an actin marker, *LifeAct-mRuby*, which clearly labeled these cytoneme-like protrusions while showing no co-localization with *tubulin-mCherry* (Figure 1D-E). Additionally, cytoneme-like protrusions were significantly reduced with cdc42 inhibitor treatment (Figure S1). Therefore, based on their cytoskeletal composition and morphology, we classified them as cytonemes.

We observed that keratinocytes marked by *krt4* expression extend cytonemes with the highest frequency during post-embryonic stages, specifically between 6.5 to 7.5 SSL (Standardized Standard Length [37]) (Figure 1C). It is worth noting that embryonic keratinocytes are replaced by post-embryonic cells around these stages, suggesting a potential role of cytonemes in epidermal remodeling and maintenance [4,37]. These keratinocyte cytonemes exhibit an approximate speed of 2.98μm/min during extension and retract at 1.9μm/min, with an average length of 18.21μm (Figure 1F-G).

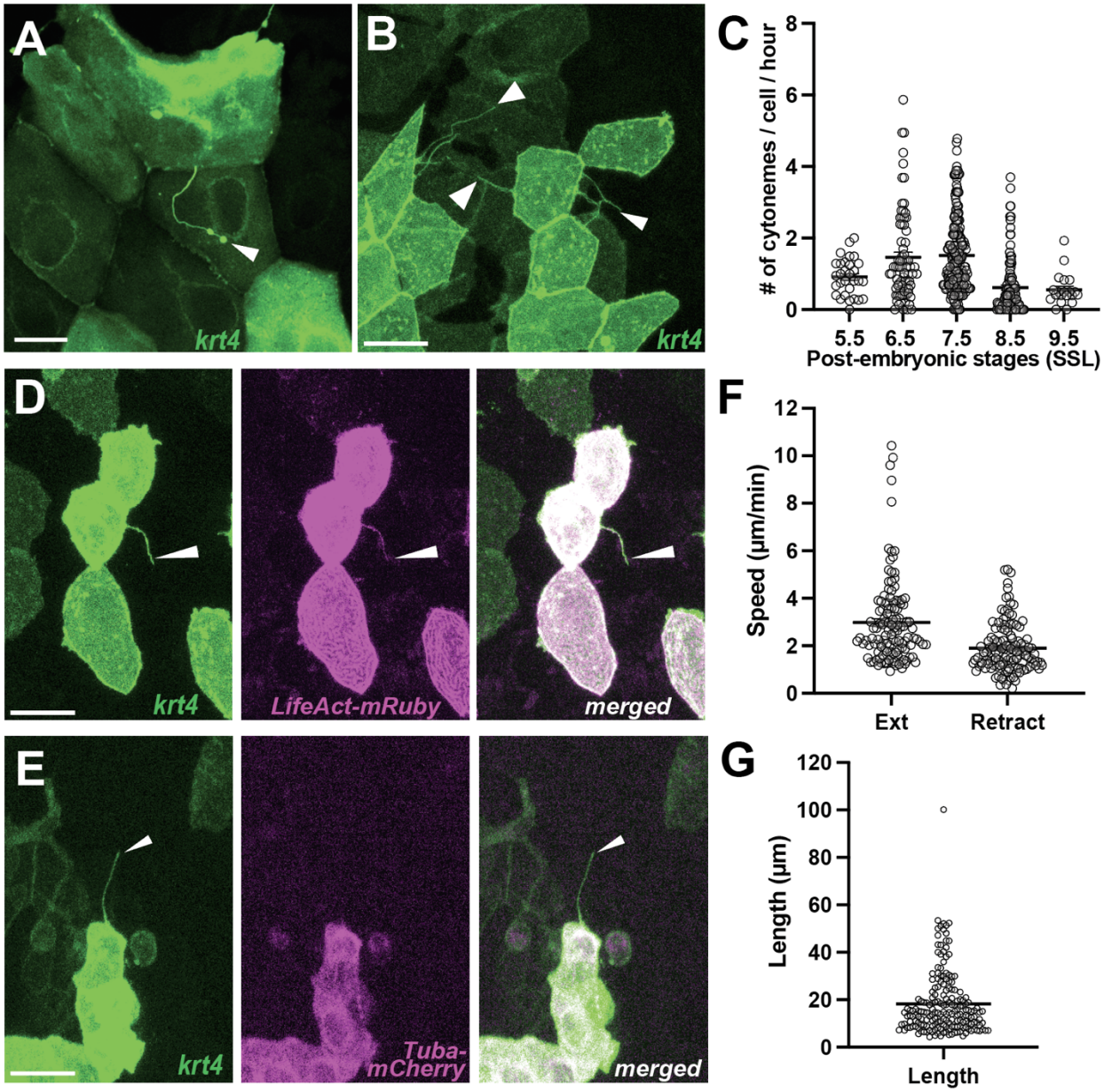

Figure 1. Differentiated keratinocytes extend cytoneme-like cellular protrusions
(A) Airineme-like protrusion (arrowhead), and (B) cytoneme-like protrusions (arrowheads) labelled in *krt4:palmEGFP* injected keratinocytes. (C) Keratinocytes expressing *krt4* extend cytoneme-like protrusions most frequently during metamorphic stages (6.5-7.5 SSL; N=457 cells, 19 larvae total). A cytoneme-like protrusion (arrowhead) labeled for (D) F-actin, revealed by *LifeAct-mRuby* but did not colocalize (E) with tubulin, revealed by *Tuba-mCherry*. (F) Keratinocyte cytonemes extend faster than they retract (N=125 cells, 4 larvae total), with an average length (G) of 18.21µm (N=190 cells, 4 larvae total). Scale bars: 20µm (A, B, D, E). Error bars indicate mean ± SEM.

Keratinocyte cytonemes establish physical contact with underlying undifferentiated keratinocytes

Similar to mammals, the zebrafish epidermis consists of three layers [2]. We specifically visualized the periderm, which is the outermost layer and consists of *krt4*+ fully differentiated keratinocytes. The intermediate layer, where undifferentiated keratinocytes reside, was marked with *krtt1c19e* promoter driving tdTomato expression, pseudo-colored in magenta [2,4]. The basal layer was also labelled with *krtt1c19e* but exhibited a typical polygonal morphology (Figure 2A-A"). This allowed us to distinguish all three epidermal layers using the *Tg(krt4:lyn-EGFP; krtt1c19e:lyn-tdTomato)*.

In addition to *krt4*+ keratinocytes, we explored whether undifferentiated keratinocytes (*krtt1c19e*+) also extend cytonemes or other types of cellular protrusions during metamorphic stages. However, we observed that cytoneme-like protrusions from undifferentiated keratinocytes were significantly fewer in numbers compared to those from fully differentiated keratinocytes, and we did not observe cytoneme-like protrusions from basal stem cells (Figure 2B-C). In this study, our focus was primarily on cytonemes from *krt4*+ differentiated keratinocytes.

To investigate the role of keratinocyte cytonemes, we first asked what the target cells of those cytonemes are. High resolution confocal imaging revealed that cytonemes originating from peridermal keratinocytes (*krt4*+) establish physical contact with underlying undifferentiated keratinocytes (*krtt1c19e*+) in the intermediate layer. Cross-sectional views showed that the tips of these cytonemes stop at the intermediate layer, with no observed instances reaching the basal layer (Figure 2D-D"', red dashed circles).

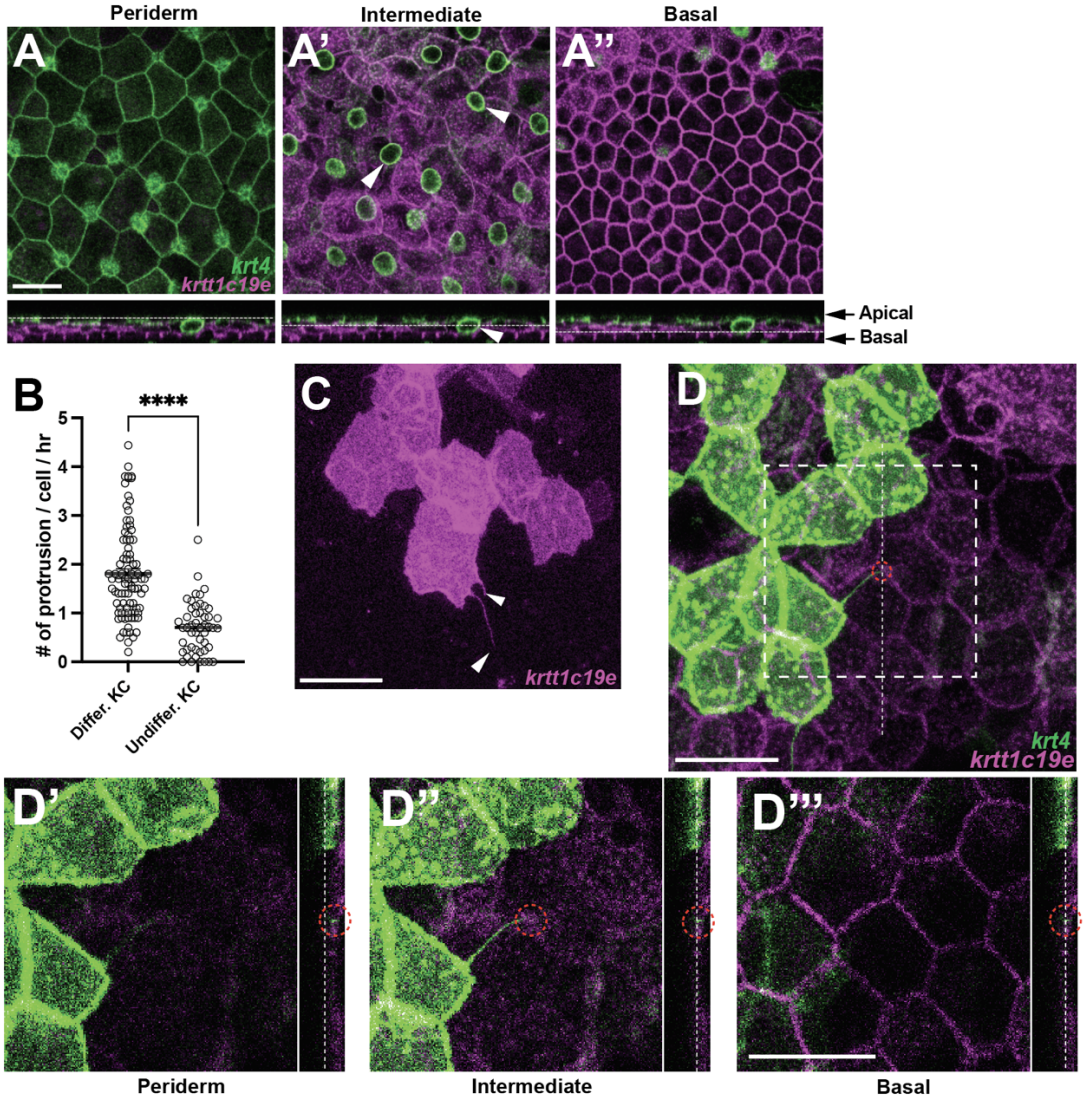

Figure 2. Keratinocyte cytonemes establish physical contact with underlying undifferentiated keratinocytes

(A-A") Postembryonic zebrafish epidermis of *Tg(krt4:lyn-EGFP;krtt1c19e:lyn-tdTomato)* comprises three distinct layers. (A) Expression of *lyn-EGFP* in *krt4*+ cells in the periderm layer. (A'-A") Expression of *lyn-tdTomato* (pseudo-colored magenta) in *krtt1c19e*+ cells in (A') the intermediate layer and (A") the basal layer. Note that the green circular labelling in (A', arrowheads) represents mucous-secreting goblet cells. [2] (B, C) Undifferentiated keratinocytes (KC) extend significantly fewer cytoneme-like protrusions (arrowheads, $P<0.0001$, N=49, 3 larvae; N=91 cells, 6 larvae total). (D-D"') Cytonemes from fully differentiated keratinocytes make physical contact with undifferentiated keratinocytes in the intermediate layer (red dotted circles). Note that dotted lines indicate the layers in the cross-sectional views. Statistical significances were assessed by Student t test. Scale bars: 20μm (A-A", C, D-D"'). Error bars indicate mean ± SEM.

Cytoneme-mediated signaling regulates keratinocyte differentiation and proliferation

The observations that cytonemes are most often observed during epidermal remodeling and their target cells are undifferentiated keratinocytes led us to hypothesize that cytoneme-mediated signaling plays a pivotal role in regulating keratinocyte differentiation and proliferation.

To test this hypothesis, we generated a transgenic line capable of temporally expressing a dominant negative form of cdc42 (cdc42DN) in peridermal keratinocytes, a strategy frequently used to inhibit cytoneme extension in various contexts [24,25]. We implemented a dually inducible TetON system in the transgene, denoted as *Tg(krt4:TetGBDTRE-v2a-cdc42DN),* and immersed the transgenic and control fish in water containing inducer drugs, doxycycline and dexamethasone, for temporal cdc42DN transgene induction [34,38]. To minimize potential off-target effects of cdc42 manipulation, we determined the drug concentrations at which normal filopodial or lamellipodial activities were maintained while inhibiting cytoneme extensions (Video S1). We employed two control groups in this experiment: one consisting of a transgenic line with no drugs and the other comprising non-transgenic fish treated with the same drug concentrations as the experimental group. Under these conditions, we observed a significant reduction in the frequency of cytoneme extension in the cdc42DN-expressing transgenic line within the drug treated group (Figure 3A-A", B). In contrast to the two control groups, the peridermal layer in the cytoneme-inhibited group displayed severe disorganization (Figure 3C-C"). Furthermore, the expression of the undifferentiated keratinocyte marker, *krtt1c19e* (magenta), was dramatically increased in the periderm when cytoneme extension was inhibited (Figure 3C-C", D). Although the cytoneme inhibition is evident after overnight treatment with the inducing drugs, noticeable epidermal phenotypes begin to appear after 3 days of treatment. This reflects the higher cytoneme extension frequency and their potential role during metamorphic stages, which takes a couple of weeks (Figure 1C) [4,37].

This co-expression of differentiated and undifferentiated keratinocyte makers in peridermal keratinocytes, along with the data that the intermediate layer is not depleted in cytoneme inhibited animals, suggests that cytoneme-mediated signal is critical for the terminal differentiation of keratinocytes (Figure 3C-D).

We mosaicly expressed *cdc42DN* in peridermal keratinocytes and observed localized disorganization in the periderm, along with co-expression of *krt4* and *krtt1c19e* in peridermal keratinocytes (Figure S3A, D, E-E'). This suggests that these defects result from the loss of cytonemes rather than broad *cdc42* inhibition. We also locally expressed other dominant-negative forms of small GTPases, such as Rac1 or Rhoab. Interestingly, *krt4*+ keratinocytes expressing dominant negative *rac1* exhibited a significant reduction in cytoneme extension and epidermal defects similar to those seen with *cdc42* inhibition, while *rhoab* manipulation showed no effects. This indicates that the observed defects are highly likely related to cytoneme loss rather than specifically to *cdc42* inhibition (Figure S3B, D, F-F'; S3C, D, G-G').

Additionally, we counted the number of peridermal keratinocytes within a 290μm x 200μm rectangle and found a substantial increase in the cytoneme-inhibited group (Figure 3E). We also confirmed that the number of Edu+ cells is significantly increased in this group (Figure 3F-G). However, it is important to note that cytoneme inhibition did

not affect the cell death rate or the number of goblet cells (Figure 3H, Figure S2A). These findings strongly suggest that cytoneme-mediated signaling controls keratinocyte differentiation and proliferation.

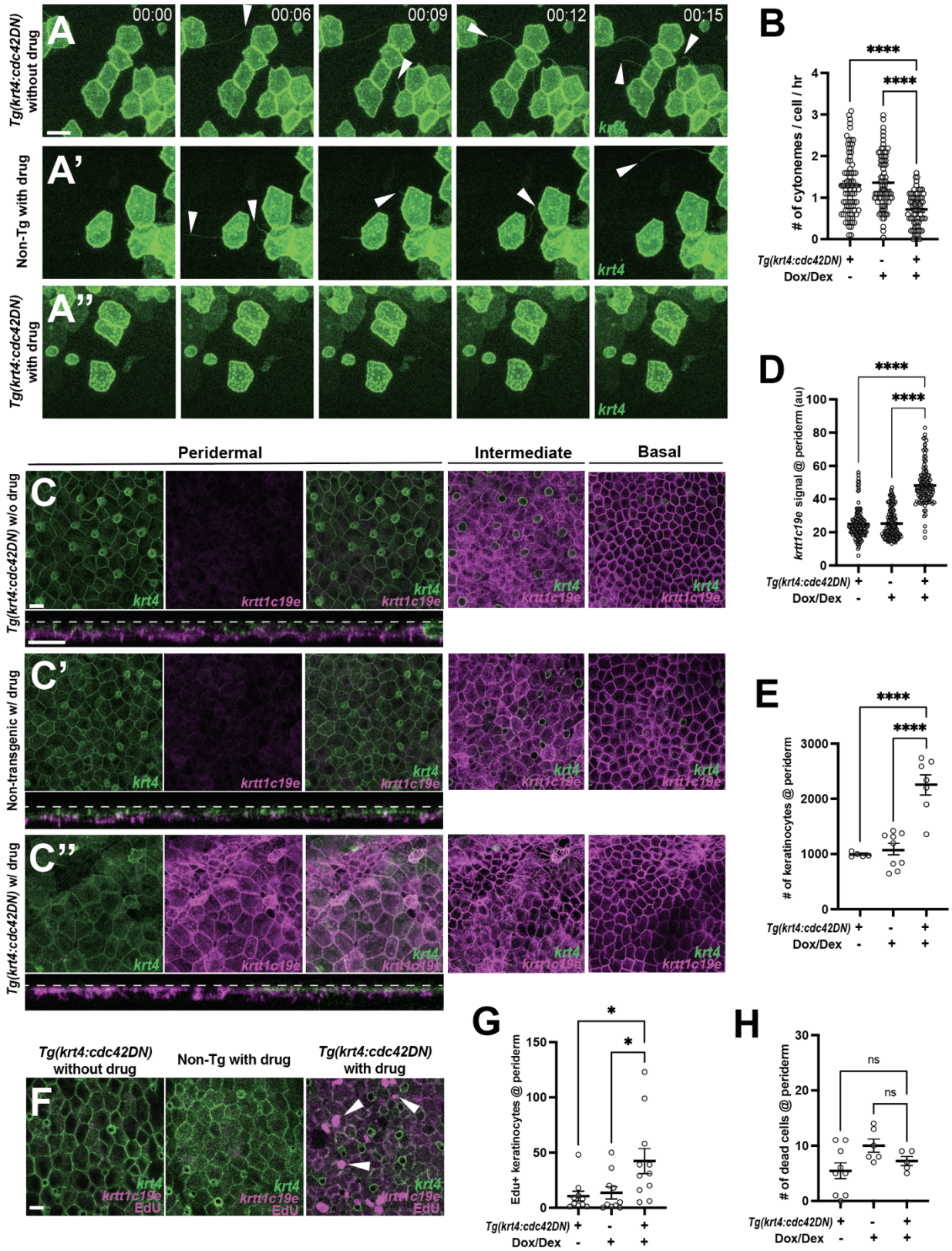
A
00:00
00:06
00:09
00:12
00:15
Tg(krt4:cdc42DN) without drug
krt4
A'
Non-Tg with drug
krt4
A''
Tg(krt4:cdc42DN) with drug
krt4
B
****
****
# of cytonemes / cell / hr
Tg(krt4:cdc42DN) + - +
Dox/Dex - + +
Peridermal
Intermediate
Basal
C
Tg(krt4:cdc42DN) w/o drug
krt4
krtt1c19e
krt4 krtt1c19e
C'
Non-transgenic w/ drug
C''
Tg(krt4:cdc42DN) w/ drug
D
****
****
krtt1c19e signal @ periderm (au)
Tg(krt4:cdc42DN) + - +
Dox/Dex - + +
E
****
****
# of keratinocytes @ periderm
Tg(krt4:cdc42DN) + - +
Dox/Dex - + +
Tg(krt4:cdc42DN) without drug
Non-Tg with drug
Tg(krt4:cdc42DN) with drug
F
krt4 krtt1c19e EdU
G
*
*
Edu+ keratinocytes @ periderm
Tg(krt4:cdc42DN) + - +
Dox/Dex - + +
H
ns
ns
# of dead cells @ periderm
Tg(krt4:cdc42DN) + - +
Dox/Dex - + +

Figure 3. Cytoneme-mediated signaling regulates keratinocyte differentiation and proliferation (A-A") Still images from time-lapse movies demonstrate that cytoneme extension (arrowheads) is inhibited in keratinocytes expressing cdc42DN. (B) Expression of *cdc42DN* effectively inhibits cytoneme extension ($F_{2, 231}$ = 25.38, P<0.0001, N=234 cells, 10 larvae total). (C) Periderm layer of *Tg(krt4:TetGBDTRE-v2a-Cdc42DN;krt4:lyn-EGFP;krtt1c19e:lyn-tdTomato)* without drug treatment. (C') Periderm layer of *Tg(krt4:lyn-EGFP;krtt1c19e:lyn-tdTomato)* with drug treatment. (C'') Periderm layer of *Tg(krt4:TetGBDTRE-v2a-cdc42DN;krt4:lyn-EGFP;krtt1c19e:lyn-tdTomato)* with drug treatment exhibits disorganization. Intermediate keratinocytes were not depleted, and basal stem cells were unaffected by the manipulation. Note that, unlike other two controls, the epidermis was not flat, resulting in partial display of basal cells in intermediate layer and dark areas in basal layer. Cross-section view exhibits *krtt1c19e* expression at the periderm. (D) Cytoneme inhibition increases *krtt1c19e* expression in the periderm ($F_{2, 387}$ = 226.7, P<0.0001, N=39 larvae total) and leads to an increased number of keratinocytes within the periderm (E) ($F_{2, 18}$ = 27.36, P<0.0001, N=21 larvae total). (F-G) Significant increase in proliferating peridermal keratinocytes in cdc42DN expressing animals ($F_{2, 28}$ = 4.888, P=0.0151, N= 9 larvae). (H) The cell death rate in the periderm is not affected by cytoneme inhibition, tested with acridine orange incorporation ($F_{2, 17}$ = 3.192, P=0.0666, N=20 larvae total). Statistical significances were assessed by One-way ANOVA followed by Tukey's HSD post hoc test. Scale bars: 20μm (A-A", C-C", F). Error bars indicate mean ± SEM.

Cytonemes activate Notch in undifferentiated keratinocytes

Previous studies have established the role of Notch signaling in controlling keratinocyte differentiation and proliferation. However, the mechanisms triggering Notch signaling in keratinocytes have remained obscure [16,39,40]. To investigate whether the target cells of cytonemes, specifically undifferentiated keratinocytes in the intermediate layer, are responsive to Notch signaling, we crossed Notch signal reporter line, *Tg(Tp1:H2B-mCherry),* with *Tg(krt4:lyn-EGFP; krtt1c19e:lyn-Tdtomato)* to label all three epidermal layers. In this Notch reporter line, the promoter from the Epstein Barr Virus terminal protein 1 (*Tp1*) gene was used as a Notch responsive element, containing two Rbp-Jκ binding sites that drive expression of Histone 2B-Cherry [41]. We observed that only undifferentiated keratinocytes in the intermediate layer exhibit Notch responsiveness, whereas keratinocytes in the periderm or basal layer do not (Figure 4A, arrowheads, Figure S4). This finding was further confirmed with immunostaining against Her6, a Notch effector, which revealed its specific expression in intermediate layer (Fig. 4B) [42]. Subsequently, we tested whether Notch activation in undifferentiated keratinocytes is dependent on cytonemes. First, we validated the *Tp1* Notch reporter line, *Tg(Tp1:EGFP)* by measuring cytoplasmic EGFP signal before and after Notch inhibitor, LY411575 treatment, which demonstrated a significant decrease in Notch signaling, as expected (Figure S5A, B). Next, we measured the difference in *Tp1* intensity before and after cytoneme inhibition. Notably, we observed a significant reduction in Notch signal under conditions where cytonemes were compromised (Figure 4C, Figure S5C). Similar to the effects on the epidermis after cytoneme inhibition (Figure 3), it takes 3 days to observe a significantly reduction in Notch signal in the undifferentiated keratinocytes. We also found more abundant Notch activated keratinocytes during metamorphic stages (Figure S5D, Figure 1C).

Next, we predicted that if cytonemes contribute to transmitting a Notch-Delta signal from differentiated keratinocytes to undifferentiated keratinocytes, then cytonemes should contain Delta ligands. Upon detecting DeltaC mRNA expression in the cytoneme

extending keratinocytes but not in its target cells (Figure S4), we investigated the localization of DeltaC protein within the cytonemes of the *krt4*+ differentiated keratinocytes. For this experiment, we utilized a construct where a 109kb BAC containing zebrafish *dlc* coding sequence regulatory elements that were recombineered to generate a mCherry fusion, resulting *dlc:Dlc-mCherry* [34]. We confirmed the presence of Dlc-mCherry along the cytonemes (Figure 4D, yellow arrowheads). These findings suggest that cytonemes are responsible for Notch activation in undifferentiated keratinocytes.

We then asked why Notch activation is dependent on cytonemes since peridermal keratinocytes and underlying intermediate keratinocytes are in constant contact with each other. We revealed that intermediate keratinocytes exclusively express *lfng* (lunatic fringe), which potentially act as a default inhibitor of Notch activation in these cells [43,44] (Figure S6). However, this needs further studies to understand how cytonemes overcome this Notch signaling barrier or potentiate the signal.

Next, we hypothesized that if Notch activation by cytonemes is essential for keratinocyte differentiation and proliferation, then direct inhibition of Notch signal in undifferentiated keratinocytes should yield phenotypes similar to those observed when cytonemes are inhibited [14]. To investigate this, we generated a transgenic line capable of temporally expressing dominant negative form of Suppressor of Hairless (SuHDN) in the undifferentiated keratinocytes, *Tg(krtt1c19e:TetGBDTRE-v2a-SuHDN)* [34]. We observed that Notch inhibition in the undifferentiated keratinocytes resulted in a disorganized periderm, abnormally increased expression of undifferentiated keratinocyte marker, and hyperproliferation of keratinocytes in the periderm (Figure 4E-E”, F-H, Figure S5C). These results closely mirrored the phenotypes observed when we inhibited cytoneme extension in peridermal keratinocytes (Figure 3C-C”, D-E, Figure S5C). These observations suggest that Notch signaling, activated by cytonemes in undifferentiated keratinocytes, plays a critical role in epidermal remodeling and maintenance.

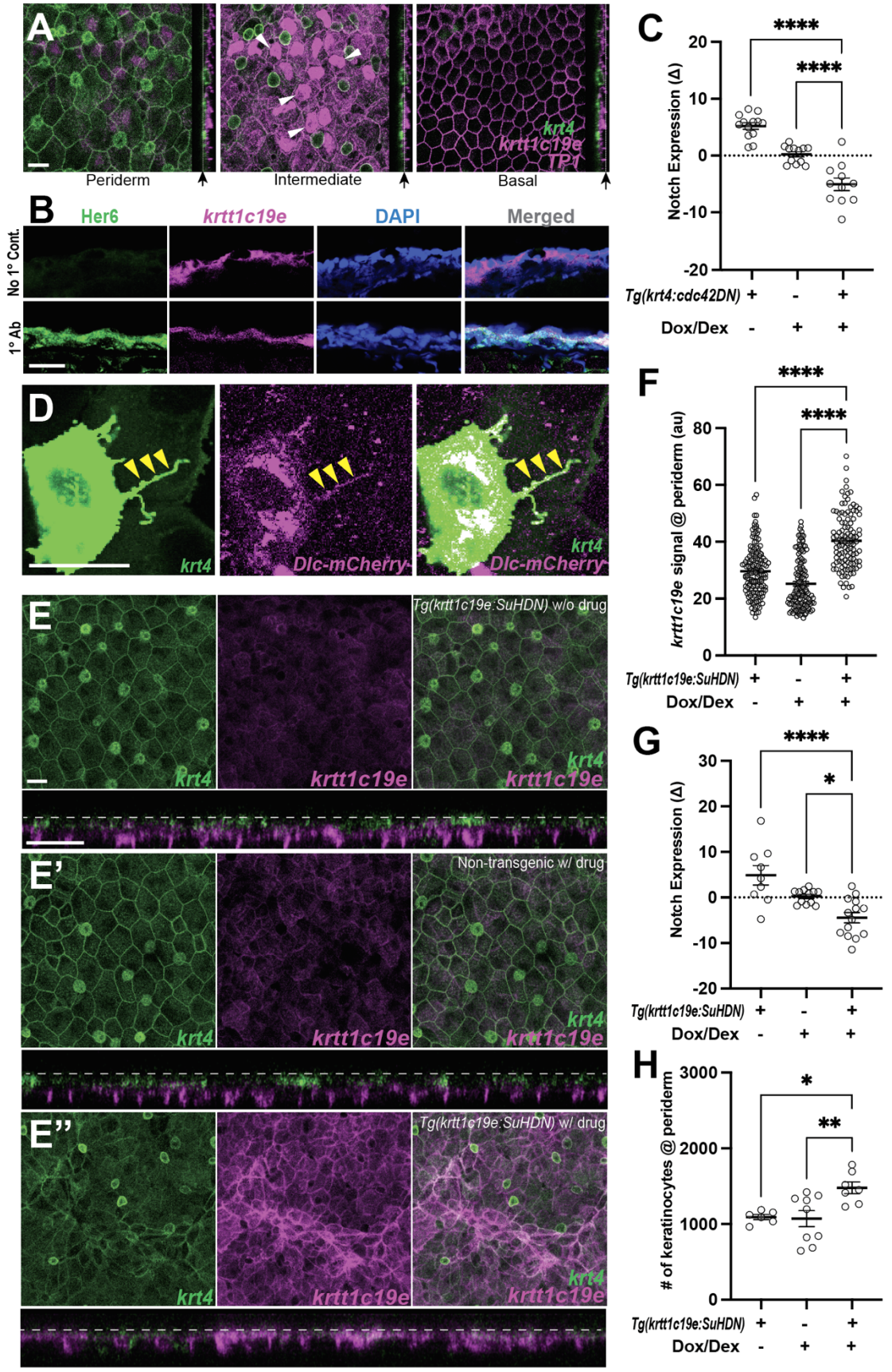
A
Periderm
Intermediate
Basal
krt4
krtt1c19e
TP-1
B
Her6
krtt1c19e
DAPI
Merged
No 1° Cont.
1° Ab
C
Notch Expression (Δ)
Tg(krt4:cdc42DN)
Dox/Dex
D
krt4
Dlc-mCherry
E
Tg(krtt1c19e:SuHDN) w/o drug
E'
Non-transgenic w/ drug
E''
Tg(krtt1c19e:SuHDN) w/ drug
F
krtt1c19e signal @ periderm (au)
G
Notch Expression (Δ)
H
# of keratinocytes @ periderm

Figure 4. Cytonemes activate Notch in undifferentiated keratinocytes
(A) Postembryonic zebrafish epidermis of *Tg(krt4:lyn-EGFP;krtt1c19e:lyn-tdTomato;TP1:H2BmCherry)* shows Notch responsiveness in undifferentiated keratinocytes within the intermediate layer but not in the periderm or basal layer. (B) Zebrafish Her6 protein expression in *krtt1c19e*+ intermediate keratinocytes. A cross-sectional view of *Tg(krtt1c19e:tdtomato)* epidermis shows that Her6 expression overlaps with the intermediate layer marker. (C) Inhibition of cytonemes reduces Notch responsiveness in undifferentiated keratinocytes ($F_{2, 33} = 48.27$, $P < 0.0001$, N=36 larvae total) (Figure S5C). (D) Expression of DeltaC-mCherry fusion protein along the cytoneme (yellow arrowheads). (E-E") Notch inhibition by expressing SuHDN in undifferentiated keratinocytes results in the disorganization of periderm (E"). (E) Properly organized periderm layer of *Tg(krtt1c19e:tetGBDTRE-v2a-SuHDN;krt4:lyn-EGFP;krtt1c19e:lyn-tdTomato)* without drug treatment and (E') *Tg(krt4:lyn-EGFP;krtt1c19e:lyn-tdTomato)* with drug treatment. (F) Notch inhibition increases *krtt1c19e* signal in the periderm ($F_{2, 397} = 89.47$, $P < 0.0001$, N=40 larvae total), (G) reduces Notch responsiveness in undifferentiated keratinocytes ($F_{2, 32} = 13.18$, $P < 0.0001$, N=35 larvae total), and leads to (H) an increased number of keratinocytes in the periderm ($F_{2, 19} = 6.620$, $P = 0.0066$, N=22 larvae total). Statistical significances were assessed by One-way ANOVA followed by Tukey's HSD post hoc test. Scale bars, 20µm (A, C, D). Error bars indicate mean ± SEM.

Interleukin-17 regulates keratinocyte cytonemes

The aberrant differentiation and hyperproliferation of keratinocytes observed when cytoneme extension was inhibited in peridermal keratinocytes (*krt4*+) or Notch signaling was inhibited in undifferentiated keratinocytes (*krtt1c19e*+) are hallmark features of many human skin diseases such as *psoriasis*, *atopic dermatitis* and more [14,46] (Figure 3, 4). Also, it has been well established that impaired Notch signaling is associated with some of these human skin disorders [7,14]. Thus, we asked which key molecules are critical for the onset or progression of these skin diseases and whether they have an impact on keratinocyte cytoneme signaling.

One of them is interleukin-17 (IL-17) and we hypothesized IL-17 signaling could influence cytoneme extension in peridermal keratinocytes. Given that IL-17 is a cytokine released into the extracellular space, and to test its role in peridermal keratinocytes, we decided to overexpress the IL-17 receptors. It is noted that interleukin-17 receptors and ligands are evolutionarily conserved across chordates [47,48].

To test, we generated transgenic lines that cell-autonomously overexpressed il17 receptor D (*il17rd*) or il17 receptor A1a (*il17ra1a*) in fully differentiated peridermal keratinocytes (*krt4*+), *Tg(krt4:nVenus-v2a-il17rd)* and *Tg(krt4:il17ra1a-v2a-mCherry)*. Both of these IL-17 receptor-overexpressing transgenic lines exhibited a significant reduction in cytoneme extension, resulting in a decreased Notch activation in undifferentiated keratinocytes (Figure 5A-C, S5E, S7A-B). Moreover, similar to the two previous manipulations, we observed a severely disorganized periderm, an upregulation of the undifferentiated keratinocyte marker expression, and hyperproliferation of keratinocytes within the periderm (Figure 5D-D”, E-H).

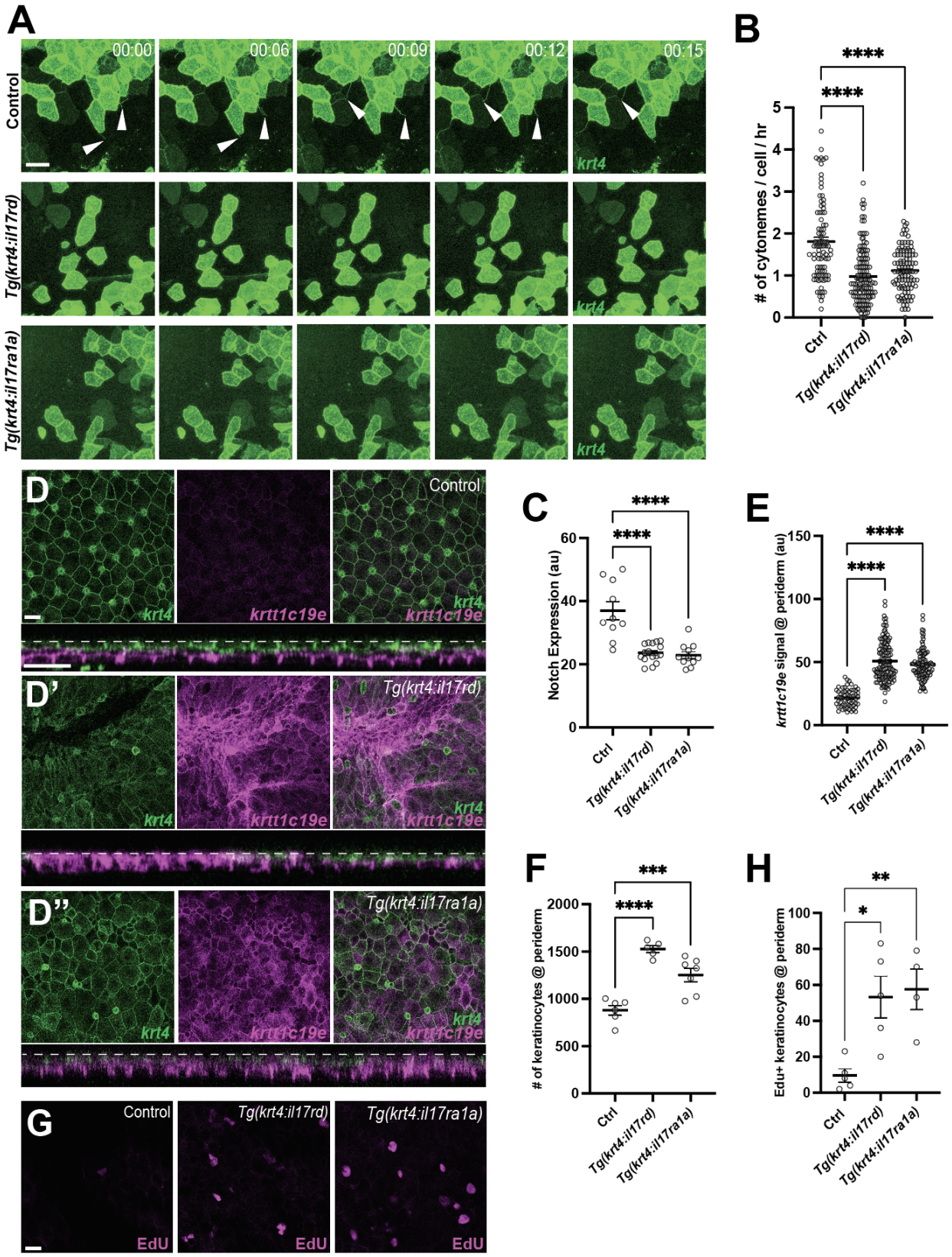
A
00:00
00:06
00:09
00:12
00:15
Control
Tg(krt4:il17rd)
Tg(krt4:il17ra1a)
krt4
B
****
****
# of cytonemes / cell / hr
Ctrl
Tg(krt4:il17rd)
Tg(krt4:il17ra1a)
D
D'
D''
krt4
krtt1c19e
Control
Tg(krt4:il17rd)
Tg(krt4:il17ra1a)
C
Notch Expression (au)
E
krtt1c19e signal @ periderm (au)
F
# of keratinocytes @ periderm
***
H
Edu+ keratinocytes @ periderm
**
*
G
EdU

Figure 5. Disruption of epidermal maintenance by Interleukin-17 receptor overexpression
Overexpression of *il17rd* or *il17ra1a* in *krt4+* keratinocytes results in (A, B) a significant reduction in cytoneme extension ($F_{2, 325}$ = 38.48, P < 0.0001, N=328 cells, 10 larvae total), and (C) decreased Notch responsiveness ($F_{2, 34}$ = 23.16, P < 0.0001, N=37 larvae total) (Figure S5E). (D-D") The periderm is disrupted in (D') *Tg(krt4:nVenus-v2a-il17rd;krt4:lyn-EGFP;krtt1c19e:lyn-tdTomato)* and (D") *Tg(krt4:nVenus-v2a-il17ra1a;krt4:lyn-EGFP;krtt1c19e:lyn-tdTomato)* compared to the (D) properly arranged periderm of *Tg(krt4:lyn-EGFP;krtt1c19e:lyn-tdTomato)*, resulting in (D', cross-section) an increased *krtt1c19e* signal in the periderm (E) ($F_{2, 287}$ = 109.7, P < 0.0001, N=29 larvae total) and (F) an increased number of keratinocytes in the periderm ($F_{2, 15}$ = 27.79, P < 0.0001, N=18 larvae total). (G, H) Edu+ peridermal keratinocytes are significantly increased in il17 receptor overexpressed larvae ($F_{2, 11}$=8.259, P=0.0065, N=14 larvae total). Statistical significances were assessed by One-way ANOVA followed by Tukey's HSD post hoc test. Scale bars: 20μm (A, D, G). Error bars indicate mean ± SEM.

To assess whether IL-17 signaling regulates keratinocyte differentiation and proliferation through cytonemes, first we overexpressed the il17a ligand in the epidermis and examined its effect on cytoneme extension. Given the abundance of tissue-resident macrophages in the epidermis, we generated a transgenic line that overexpressed *il17a* under a macrophage promoter, *Tg(mpeg1:il17a-v2a-mCherry)* (Figure S7C) [33]. Consistent with the experiments that overexpressed il17 receptors, we confirmed that il17a ligand overexpression in the epidermal microenvironment led to a significant reduction in cytoneme extension in the differentiated keratinocytes (Figure 6A-B). Next, we generated an *il17a* loss-of-function mutant using CRISPR/Cas9 approach. This mutant harbor an 11bp deletion in the second exon of the *il17a* gene, resulting in a premature stop codon (Figure S8). We observed a significant increase in cytoneme extension frequency in *il17a* heterozygote or homozygote mutants as compared to their wild-type siblings (Figure 6C-D). Together, our findings suggest that IL-17 signaling controls cytoneme extension.

Subsequently, we sought to understand how the IL-17 signal impacts cytoneme extension. Studies have shown that IL-17 signaling can regulate actin cytoskeleton in keratinocytes [49,50]. To evaluate whether *il17rd* or *il17ra1a* overexpression alters the actin cytoskeleton and consequently cytonemes, we compared keratinocyte microridges, which are actin cytoskeleton-rich structures, between control and *il17rd*- or *il17ra1a* overexpressed peridermal keratinocytes [51,52]. We first confirmed that overexpression of *cdc42DN* or *rac1DN* disrupts microridge formation in differentiated keratinocytes (Figure S9). Our observation revealed severe disorganization of microridges in the keratinocytes overexpressing *il17rd- or il17ra1a*. This was coupled with a significant down-regulation of *Cdc42* and *Rac1* GTPase expression in these cells (Figure 6E-G). These data suggest that IL-17 signaling negatively regulates cytoneme extension by down-regulating *Cdc42* and *Rac1*, which are essential for controlling the actin cytoskeleton (Figure S3, S9) [25,53-55].

We then crossed two transgenic lines: *Tg(krt4:TetGBDTRE-v2a-cdc42DN)* and either *Tg(krt4:nVenus-v2a-il17rd)* or *Tg(krt4:il17ra1a-v2a-mCherry)*. Given that il17 receptor overexpression reduced *Cdc42* expression in differentiated keratinocytes (Figure 6E), we anticipated observing a more severe inhibition of cytoneme extension when these manipulations are combined compared to individual manipulations. Indeed, when inhibited cytoneme extension with the *cdc42DN* along with *il17rd* or *il17ra1a*

overexpression, we observed a more significant inhibition of cytoneme extension than when manipulated individually (Figure 6H).

Our data collectively support the idea that cytoneme-mediated intercellular signaling between peridermal and underlying undifferentiated keratinocytes is essential for epidermal remodeling and maintenance. IL-17 functions as a regulator capable of affecting cytoneme extension by modulating the actin cytoskeleton in keratinocytes. Consequently, our data suggest that the overproduction of IL-17 ligands by immune cells in conditions such as psoriatic or other skin diseases leads to epidermal imbalance through altered cytoneme signaling in keratinocytes.

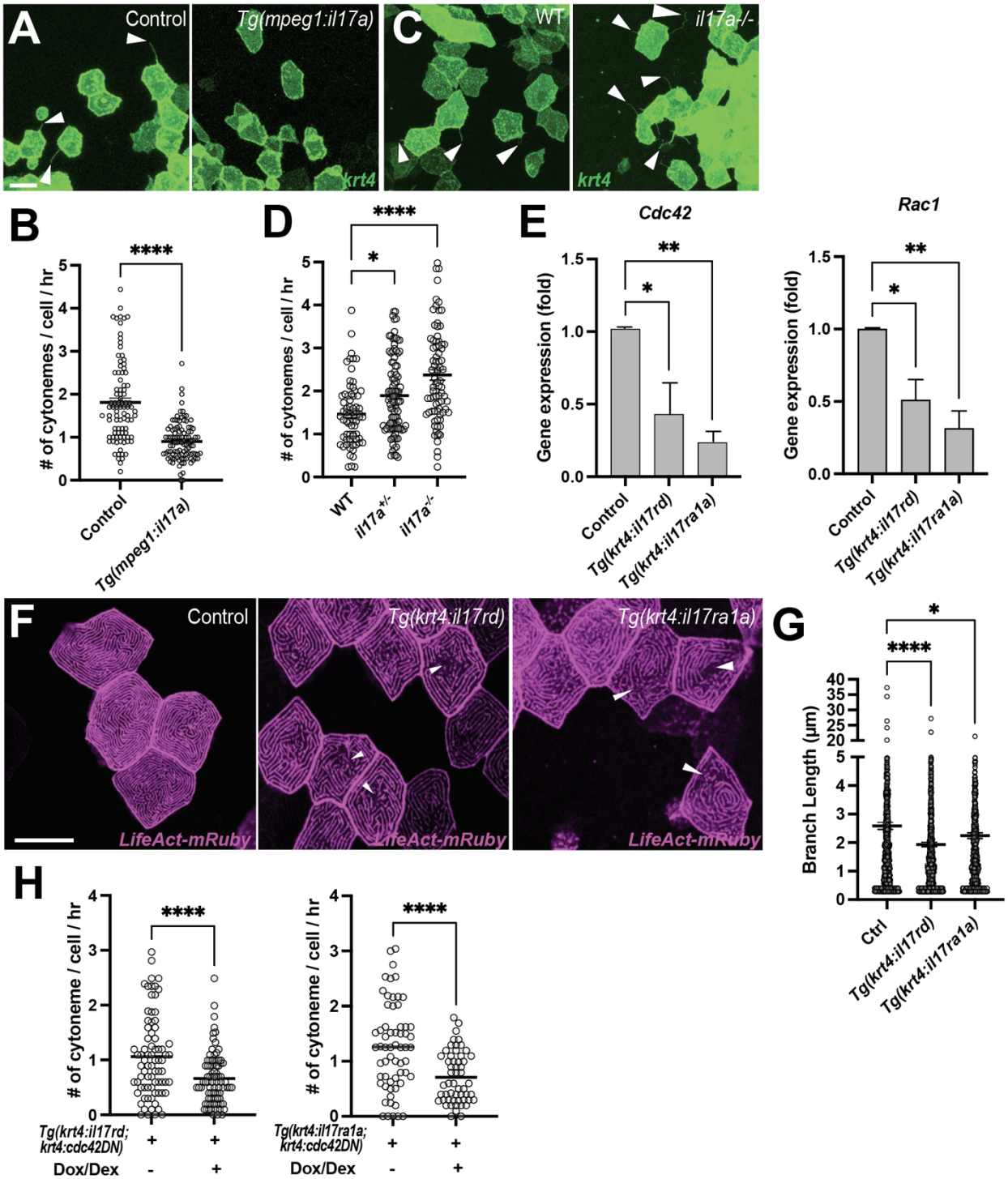
A
Control
Tg(mpeg1:il17a)
krt4
C
WT
il17a-/-
krt4
B
# of cytonemes / cell / hr
****
Control
Tg(mpeg1:il17a)
D
# of cytonemes / cell / hr
****
*
WT
il17a+/-
il17a-/-
E
Cdc42
Rac1
Gene expression (fold)
**
*
Control
Tg(krt4:il17rd)
Tg(krt4:il17ra1a)
F
Control
Tg(krt4:il17rd)
Tg(krt4:il17ra1a)
LifeAct-mRuby
G
Branch Length (µm)
*
****
Ctrl
Tg(krt4:il17rd)
Tg(krt4:il17ra1a)
H
# of cytoneme / cell / hr
****
Tg(krt4:il17rd; krt4:cdc42DN)
Tg(krt4:il17ra1a; krt4:cdc42DN)
Dox/Dex
-
+

Figure 6. Interleukin-17 regulates keratinocyte cytonemes
(A) Representative images of *krt4:palmEGFP* injected cells in control or *Tg(mpeg1:il17a).* (B) Significant reduction in cytoneme extension in response to overexpressed il17a ligands in the epidermis (P<0.0001, N=3 larvae per group). (C) Representative images of *krt4:palmEGFP* injected keratinocytes in WT or *il17a-/-* mutants. (D) Cytoneme extension frequency increased significantly in *il17a*$^{+/-}$ or *il17a*$^{-/-}$ mutants as compared to their wild-type siblings ($F_{2, 247}$=17.85, P<0.0001, N=250 cells, 9 larvae total). (E) FACS-sorted *krt4+* peridermal cells from *Tg(krt4:palmEGFP; krt4:il17rd)* or *Tg(krt4:palmEGFP; krt4:il17ra1a)* show significantly reduced *Cdc42* (P= 0.0341 for *il17rd*, P=0.01 for *il17ra1a*, N=3 independent experiments) and Rac1 expression (P=0.0189 for *il17rd*, P=0.0017 for *il17ra1a*, N=4 independent experiments). (F) *il17rd*-or *il17ra1a* overexpressing *krt4+* keratinocytes exhibit disorganization of microridges (arrowheads), with (G) significantly reduced branch lengths of microrides in the transgenic animals ($F_{2, 2311}$=11.11, P<0.0001, N=68 cells, 9 larvae total). (H) Simultaneous overexpression of *cdc42DN* and *il17rd* or *il17ra1a* in *krt4+* keratinocytes further reduces cytoneme extension (*il17rd*: P < 0.0001, N=164 cells, 7 larvae total, *il17ra1a*: P < 0.0001, N=115 cells, 6 larvae total). Statistical significances were assessed by One-way ANOVA followed by Tukey's HSD post hoc test or Student t test. Scale bars: 20μm (A, C, F). Error bars indicate mean ± SEM.

In addition, recent human Genome-Wide Association Studies (GWAS) have identified a close association between *clint1* and individuals with *psoriasis* and *atopic dermatitis* [32]. The clathrin interactor 1 (*clint1*), also referred to as enthoprotin and epsinR functions as an adaptor molecule that binds SNARE proteins and play a role in clathrin-mediated vasicular transport [56]. It has also been reported that *clint1* is expressed in epidermis and play an important role in epidermal homeostasis and development in zebrafish [31]. Given these reported findings, we investigated to determine whether *clint1* plays a role in epidermal maintenance through its influence on keratinocyte cytonemes. Indeed, we found that *clint1* mutants exhibited a significant decrease in cytoneme extension in peridermal keratinocytes, accompanied by reduced Notch signaling in undifferentiated keratinocytes. As a result, these mutant fish displayed abnormal keratinocyte differentiation and hyperproliferation of keratinocytes (Figure S10). These findings suggest that *clint1* is yet another regulator of cytoneme-mediated intercellular signaling in keratinocytes.

In conclusion, the intercellular signaling facilitated by cytonemes between fully differentiated and undifferentiated keratinocytes is crucial for the maintenance and remodeling of the epidermis. Our study implies that the patients with human skin diseases may have defective cytoneme signaling between keratinocytes.

Discussion

It is intriguing to observe that keratinocytes have the ability to extend both cytoneme and airineme-like protrusions. While these protrusions differ in their extension frequency and developmental context, this observation implies that a single cell type can employ two distinct types of cellular protrusions for signaling, each capable of transferring unique signaling molecules to potentially different targets. Previous research in *Drosophila* has demonstrated that the air sac primordium (ASP) can extend multiple cytonemes that appear morphologically identical but convey different signaling molecules [57]. However, it remains unknown whether the same cell type can extend two morphologically (and functionally) distinct protrusions that might also serve distinct functions in separate contexts. Consequently, future studies aimed at unraveling the regulation of these two types of protrusions could provide insights into how cells choose their signaling modalities based on their specific signaling requirements and environmental cues.

We have asked why cytoneme-mediated signaling is necessary between fully differentiated- and undifferentiated keratinocytes, even though they are separated by opposing cell membranes. Notably, we have identified the Notch signaling pathway as being involved, which operates through membrane receptor and ligand interactions between adjacent cells. This led us to hypothesize that Notch signaling between cells in these layers is suppressed by Fringe proteins, which modulate Notch signaling. In our research, we have discovered that *lunatic fringe (lfng)* is exclusively expressed in the intermediate layer in zebrafish ([44], Figure S6). Early studies in mice have also reported that three fringe genes exhibit differential expression in different epidermal layers [58]. Hence, it appears that Notch signaling is tightly regulated or inhibited by default between epidermal layers in both zebrafish and mice. While it is well documented that Notch signaling is essential for keratinocyte differentiation and proliferation, the mechanism by which Notch signaling is initiated remains unclear. Our study suggests that cytonemes from fully differentiated keratinocytes in the periderm can activate Notch signaling in undifferentiated keratinocytes in intermediate layer. However, further investigations are necessary to fully comprehend how cytoneme-mediated signaling coordinate with Lunatic fringe or other Fringes to trigger the Notch signal.

It is widely believed that the overproduction of IL-17 is a major contributing factor to *psoriasis*, and many studies have demonstrated that IL-17 signaling triggers inflammation [59]. IL-17 affects various cellular targets, such as keratinocytes, neutrophils, endothelial cells, promoting tissue inflammation [60]. Thus, further studies are essential to determine whether uncontrolled cytoneme-mediated signaling in keratinocytes correlates with the onset or progression of psoriatic or other skin diseases. Nevertheless, our data strongly indicate that cell-autonomous overexpression of *il17rd* in peridermal keratinocytes (*krt4*+) can induce psoriasis-like phenotypes by inhibiting cytoneme extensions, which subsequently leads to a reduction in Notch signaling in undifferentiated keratinocytes. A diminished Notch signal has been observed in psoriatic lesions [15]. Our study suggests that cytoneme-mediated intercellular communication between keratinocytes plays a crucial role in epidermal maintenance, and its dysregulation may contribute to the development of human skin diseases. This idea has yet to be fully appreciated, and it could open up new avenues for understanding the onset or progression of human skin diseases.

Moreover, we have demonstrated that IL-17 can influence cytoneme extension by regulating Cdc42 GTPases, ultimately affecting actin polymerization. Consequently, it would be intriguing to investigate whether genes associated with *psoriasis* or other human skin diseases also function as regulators of cytonemes. For instance, the epidermal-specific deletion of inhibitor of NF-kB kinase 2 (IKK2) or the double knock out of the c-Jun and JunB genes in mice resulted in psoriasis-like phenotypes in a T cell-independent manner [61,62]. Among the various roles of IKK and JunB, they are also known to regulate the actin cytoskeleton [63-65]. Thus, it is conceivable that dysregulated cytoneme-mediated signaling may contribute to psoriatic conditions in these contexts. Similarly, we have shown that *clint1* mutants exhibited compromised cytoneme signaling and keratinocyte hyperproliferation (Figure S10) [31]. Clint1(Clathrin Interactor 1) plays an important role in vesicle trafficking, and it is suggested that endocytic pathways are critical for multiple steps in cytoneme-mediated morphogen delivery [25,66]. Therefore, it is interesting to investigate whether clint1 functions as a cytoneme regulator could provide valuable insights.

Another important question requires an answer: the proper remodeling and maintenance of the epidermis seemingly depend on a well-controlled supply of keratinocytes from basal stem cells. Our study demonstrated the relay of cytoneme-mediated signals from the periderm to the underlying undifferentiated keratinocytes, leading to their differentiation and subsequent replacement of peridermal keratinocytes. However, the mechanism through which basal stem cells detect the need for an increased population of keratinocytes to maintain the intermediate layer remains unclear. This process does not necessarily involve cellular protrusion-mediated signaling. However, we discovered cytoneme-like protrusions originating from undifferentiated keratinocytes (Figure 2B-C). Our preliminary data, not presented in this manuscript, suggests that these cellular protrusions project downward, indicating their interaction with basal stem cells. Although further investigation is needed, it is conceivable that a replenishment signal from external sources or the periderm can be transmitted to stem cells through a multi-step cytoneme-mediated intercellular signaling pathways.

Acknowledgements
We thank Drs. Plikus, Andersen and Parsons for the invaluable discussions, and all the members of Eom lab for maintaining our fish lines. This study was supported by the National Institutes of Health grant R35GM142791 (to D.S.E.) and National Institutes of Health T32 training grant AR080622 (to Y.W.).

Author Contributions
Conceptualization, Y.W. and D.S.E.; Investigation, Y.W., T. N., Q.H., O.H., K.F. and D.S.E.; Writing – Original Draft, Y.W. and D.S.E.; Writing – Review & Editing, Y.W. and D.S.E.; Funding Acquisition; D.S.E. and Y.W.; Supervision, D.S.E.
Competing interests
The authors declare no competing interests.

EXPERIMENTAL MODEL AND SUBJECT DETAILS

Zebrafish
Adult zebrafish were maintained at a constant temperature of 28.5°C under a 16:8 (L:D) cycle. The zebrafish used in this study were wild-type AB^{wp} or its derivative WT(ABb). Additionally, transgenic lines used include *Tg(krt4:lyn-EGFP)*^{sq18}*, Tg(krtt1c19e:lyn-tdTomato)*^{sq16} provided by T. Carney; *Tg(Tp1:EGFP)*^{um13}*, Tg(Tp1:H2BmCherry)*^{jh11} provided by M. Parsons*; clint1a*$^{hi1520Tg/+}$*(AB),* obtained from the Zebrafish International Resource Center (ZIRC). The sexes of individual fish could not be distinguished since experiments were performed before developing secondary sexual characteristics. All zebrafish stocks used in this study were known to produce balanced sex ratios, ensuring that experiments sampled similar numbers of males and females. All animal work conducted in this study received approval from the University of California Irvine Institutional Animal Care and Use Committee (protocol #AUP-25-002) and adhere to institutional and federal guidelines for the ethical use of animals.

METHOD DETAILS

Transgenesis and transgenic line production
Transgenic fish lines with cell-type specific and temporally inducible expression of human *cdc42DN* and *SuHDN* were generated following the protocol described by Eom et al., (2015). These constructs were driven by a 2.2kb *krt4* promoter obtained from T. Carney for the expression in fully differentiated keratinocytes and a 3.9kb *krtt1c19e* promoter, also from T. Carney, for the expression in undifferentiated keratinocytes and epidermal stem cells. The efficiency of gene expression in both *Tg(krt4:TetGBDTRE-v2a-cdc42DN)*$^{ir.rt3}$ and *Tg(krtt1c19e:TetGBDTRE-v2a-SuHDN)*$^{ir.rt18}$, induced by doxycycline (Dox; Sigma-Aldrich) and dexamethasone (Dex; Sigma-Aldrich), was performed in both F0 mosaic fish and non-mosaic stable lines, with consistent results. The coding sequence of *il17rd* (ZDB-GENE-020320-5) and *il17ra1a* (ZDB-GENE-070705-242) were isolated from WT(ABb) cDNA and used to generate constructs driven by the *krt4* promoter, which were assembled using Gateway assembly into the pDestTol2CG2 destination vector to produce *Tg(krt4:nVenus-v2a-il17rd)*$^{ir.rt16}$ and *Tg(krt4:il17ra1a-v2a-mCherry)*$^{ir.rt17}$. Similarly, *Tg(mpeg1:il17a-v2a-mCherry)*$^{ir.rt21}$ was produced by isolating the coding sequence of il17a (ZDB-GENE-061031-3) from WT(ABb) cDNA and using Gateway assembly to assemble the construct driven by the mpeg1 promoter into the pDestTol2-exorh:mCherry destination vector [Addgene #195989]. The lunatic fringe reporter line, *Tg(lfng:mCherry)*$^{ir.rt20}$, was generated by first amplifying the *lfng* promoter sequence (ZDB-GENE-980605-16) using WT gDNA and then used Gateway assembly into the pDestTol2-exorh:EGFP destination vector [Addgene #195983]. These constructs were then injected into WT(ABb) fish to generate mosaic F0 fish, which were then bred in pairs to find germline carriers to produce non-mosaic transgenic lines. Actin was examined with *LifeAct-mRuby* [Addgene #166977] [67] driven by *krt4* promoter. Microtubules in *krt4*+ keratinocytes and cytonemes were labelled using subclones from Tuba1-mCherry [(Addgene #49149] [68].

Generation of *il17a* mutants by the CRISPR/Cas9 System

Disruption of *il17a/f1* (GenBank accession number NM_001020787) was performed using CRISPR/Cas9 technology. The target site in exon 2 was selected using SMART and the corresponding sequence was 5'-AGCAGATCATTCATACCGGC-3'. Single guide RNA (sgRNA) was synthesized using MEGAshortscript™ T7 High Yield Transcription Kit (Invitrogen). Then, 1µg/µL TrueCut™ Cas9 Protein v2 (Invitrogen™) and 300ng/µL sgRNA were co-injected into the one-cell stage zebrafish embryos to knockout the *il17a* gene. Founder fish (F0) were outcrossed with WT(ABb) to generate *il17a* heterozygous mutants, which were identified upon adulthood and intercrossed to obtain *il17a* homozygote mutants. The PCR primers for genotyping were as follows: Forward 5'- CCTCCGCTTTCTTATGGTGAGTATAGC -3' and Reverse 5'- GGAACCACTGAATGCCAATATAGCAG -3'.

Drug treatments

Zebrafish were kept in E3 medium with or without drugs (Dox/Dex) during both the light and the dark cycles for long-term drug treatment experiments. For overnight time-lapse images, fish subjected to drug-treatment were transferred to fresh E3 medium 30min before explant preparation to minimize background fluorescence from the drugs. Zebrafish with *krt4:palmEGFP* injected TetGBD-containing transgenics and non-transgenic siblings were treated with 37.5µM Dox and 50µM Dex one day prior to time-lapse imaging, while fish for long-term (3-day) drug treatment received 27.5 µM Dox and 50µM Dex starting from SSL7.0.
Notch inhibitor, LY411575 (10mM; Thomas Scientific) was prepared in DMSO (Sigma-Aldrich), and fish were treated with drug [LY411575 (3µM)] or vehicle from SSL7.0. For acute drug administration, Cdc42 inhibitor ML141 (Sigma-Aldrich), prepared in DMSO, was added to fish medium [ML141 (2µM)] 30min prior to explant preparation for time-lapse imaging.

Acridine Orange Cell Death Assay

Acridine Orange (5mg/mL; Sigma-Aldrich) was prepared in Invitrogen UltraPure™ Distilled Water. Fish were washed in 1x E3 medium 30min before being transferred to 1x E3 medium containing AO (2µg/mL). The fish were incubated in AO for 30min and then rinsed in regular 1x E3 medium three times for 10min each to minimize background fluorescence during imaging. Dead cells, pseudo-colored in magenta, were counted for all groups.

Time-lapse and still imaging

Ex vivo time-lapse imaging of zebrafish epidermal cells within their native tissue environment was acquired at 3-minute intervals for 10 hours. This was achieved using a 40x water-immersion objective on a Leica TCS SP8 confocal microscope equipped with a resonant scanner and two HyD detectors. Larvae were imaged at SSL7.5, unless otherwise specified. For still images, the region directly underneath the dorsal fin of the zebrafish was captured, with a total of 10 tiles per fish.

Cytoneme Analysis

In zebrafish keratinocytes, lamellipodial extensions are the dominant extension type, and most filopodial extensions are less than 1µm in length, both are not easily visible at

the confocal resolution we used for this study. Thus, it is easy to distinguish filopodia from cytonemes, as cytonemes have a minimum length of 4.36μm in our observations. We did not use the width parameter since there are no other protrusions except cytonemes. We calculated the cytoneme extension frequency by counting how many cytonemes extended from a cell per hour. We analyzed movies with 3-minute intervals over a total of 10 hours, as described in the section above.

RT-PCR, qRT-PCR and FACS

Zebrafish at SSL7.5 were skinned (N=15 per group), and the dissected tissues were placed in cold 1x PBS. Tissues were washed by pipetting up and down and then centrifuged to remove the supernatant. Next, 1mL Gibco Stem® Pro® Accutase Cell Dissociation Reagent was added to resuspend tissues, and the tube was incubated for at least 10 min at 37°C to dissociate the cells. After incubation, the cells were passed through 40μm cell strainers to remove large tissue chunks before subjecting them to FACS (Fluorescence-activated cell sorting). FACS enabled the separation and collection of desired cell populations based on different cell membrane markers. EGFP+ and tdtomato+ cells were collected for downstream non-quantitative RT-PCR and quantitative RT-PCR. For cDNA synthesis, the Invitrogen Cells Direct™ One-Step qRT-PCR Kit was employed. Quantitative PCR was conducted on an Applied Biosystems QuantStudio™ 3 Real-Time PCR Instrument using PowerUP SYBR Green Master Mix and custom primers. *actb1*: 5'- CATCCGTAAGGACCTGTATGCCAAC- 3', 5'- AGGTTGGTCGTTCGTTTGAATCTC- 3' (Hu et al., 2016); *il17rd:* 5'- AAATGCAGCTATAAGCAGGGA -3', 5'- ATGTGACTCCGAGTTTGCGA -3'; *il17ra1a*: 5'- TGTAAGCACTGAAGCCGATGT -3', 5'- CACATCGAGGATGCGGAAGT -3'; *il17a/f1*: 5'- GATAGACGGCGTTGAGGTCC -3', 5'- TCCACATAAGGACGAACGCA -3'; *cdc42*: 5'- ATACGTGGAATGCTCCGCTC -3', 5'- ACGCTTCTTCTTGGGCTCTG -3';; *rac1*: 5'- AGGCCATAAAGTGTGTGGTCGTC -3', 5'- GTAGGAAAGCGGTCGAAGCCTGTC -3'. Quantitative PCRs were run with at least triplicate biological and technical replication for each sample.

Non-quantitative RT-PCR amplifications were performed with 40 cycles (*actb1, dlc, krt4, krt19, notch1a, notch2, notch3*) using Takara PrimeStar GXL DNA Polymerase. *actb1*: 5'- CATCCGTAAGGACCTGTATGCCAAC- 3', 5'- AGGTTGGTCGTTCGTTTGAATCTC- 3' (Hu et al., 2016); *krt4*: 5'- TCAACCAGGTCTATCTCTTACTCC- 3', 5'- AACAGGCTCTGGTTGACAGTTAC- 3'; *krt19*: 5'- GCTACCACCTTCTCCAGCGGAAG- 3', 5'- TGCAGCACCAAATCCTCCACCAG- 3'; *dlc*: 5'- CGGGAATCGTCTCTTTGATAAT- 3', 5'- CTCACCGATAGCGAGTCTTCTT- 3'; *notch1a*: 5'- CGGCATCAACACCTACAACTG- 3', 5'- TGGACACTCGCAGAAGAAGG- 3'; *notch2*: 5'- GAGTGTGTGGACCCGTTAGTATG- 3', 5'- GCAGGCATCATCAATGTGACAC- 3'; *notch3*: 5'- TCAGGATTGTTCTCTCGTTGATG- 3', 5'- GTGTTAAAGCATGTACCACCATTG- 3'.

Cell Counts

For all experiments, 6 out of 10 tiles of still images, which represent the central trunk area directly beneath the dorsal fin, were selected for cell counts. To ensure consistency across all samples and minimize discrepancies resulting from variations in

fish trunk widths, a region of interest (ROI), 290μm x 200μm per tile, was created using the rectangle selection tool in ImageJ. Z-stack imaging was confined to the superficial/periderm layer based on the cross-sectional view, and the final count included both *krt4*+ and *krtt1c19e*+ cells at the periderm layer.

Intensity analyses

To analyze Notch expression level, tile images were merged separately for each fish. Merged images were then sectioned in ImageJ using the polygon selection tool to encompass only the fish trunk, and maximal projection was utilized to obtain the mean gray value. For *krtt1c19e*+ expression in the periderm layer, the z-stack was set as previously described, and the mean gray value of *krtt1c19e*+ expression was obtained.

Microridge Length Analysis

The workflow for microridge length analysis was modified from van Loon et al., 2020 [52]. In brief, raw images obtained from the Leica TCS SP8 confocal microscope were imported into ImageJ with z stacks adjusted to include only the cell of interest. The cell outline was traced by the polygon tool and the area around the cell was cleared. Then the segmented cell was converted into grayscale followed by automatic adjustment of Brightness and Contrast. Images were then sharpened once, and a Gaussian Blur filter was applied with a 0.5 Sigma (Radius) before converting into a binary format for skeletonization. Branch lengths were calculated by the Analyze Skeleton (2D/3D) feature.

Western blotting

Total protein was obtained from adult zebrafish tissues with the protocol modified from Xue et al., 2022 [69]. In brief, tissues were homogenized in 200 μL cold NP-40 Lysis buffer (BP-119X; Boston BioProducts, Inc.) with 1x protease inhibitor cocktail (539131; Sigma-Aldrich). The homogenates were incubated on ice for 30min before centrifuging at 14,000 x g at 4°C for 30min. 5 μL of the supernatants were used to quantify total protein with the BCA protein assay. The supernatants were then subjected to SDS-PAGE and transferred to PVDF membranes. The primary antibody used was Rabbit anti-IL-17 a/f1 at 1:1000 (KP1239Z-100; KINGFISHER BIOTECH, INC.) and Rabbit anti-β-actin at 1:5000 (GTX637675 ; GeneTex). The secondary antibody used was anti-rabbit IgG, HRP-linked Antibody #7074; Cell Signaling TECHNOLOGY). The experiments were performed in triplicates and representative results are shown.

5-Ethynnyl-2'-deoxyuridine (EdU) labeling

The Click-iT™ EdU Cell Proliferation Kit (Thermo Fisher) was used to label DNA of proliferating cells with AlexaFluor-594. The protocol was modified for zebrafish as follows: zebrafish larvae with desired transgenic backgrounds were raised to SSL7.5 or treated with drugs as described earlier and incubated in EdU solution (500 uM in E3) at 28°C for at least 2hr. Larvae were fixed in 3.7% Formaldehyde in PBS overnight then washed and transferred to permeabilization solution, 0.5% TritonX-100 in PBS for 1 h. Permeabilized larvae were then treated according to manufacturer protocol. Proliferating cells were defined as cells that are positive for EdU.

Immunohistochemistry

The protocol was modified from Abcam IHC-Frozen protocols. Zebrafish larvae were raised to desired developmental stages. A fresh transplant was prepared from the trunk and frozen in O.C.T. Tissues were sectioned according to the protocol and immediately fixed with 4% PFA for 10 minutes at room temperature then washed with 1x PBS. Samples were permeabilized in 0.2% Triton in 1xPBS for 10 minutes and blocked in 10% Normal Goat Serum for 1 hr at room temperature. The primary antibody used was Rabbit anti-Hes1(MA5-32258; Invitrogen). Primary antibodies were diluted in 10% Normal Goat serum (50197Z; Thermo Fisher) 1:250 and samples were incubated overnight at 4°C. Samples were washed with 1xPBS. The secondary antibody used was Donkey Anti-Rabbit IgG H&L Alexa Fluor® 488 (ab150073; Abcam). Secondary antibodies were diluted 1:250 in 10% Normal Goat Serum and samples were incubated for 1 hr at room temperature and washed with fresh 1x PBS. DAPI Fluoromount-G® (0100-20; SouthernBiotech) was used to mount coverslip and prepared according to manufacturer protocol.

QUANTIFICATION AND STATISTICAL ANALYSIS

GraphPad Prism software version 9.0.0 for Windows (GraphPad Software, San Diego, CA, USA) was used to perform statistical analyses. Continuous data were evaluated by Student t-test and Post hoc means were compared by Tukey-Kramer HSD.

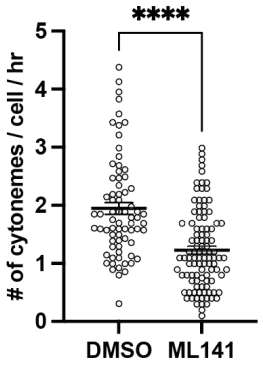

Figure S1. Effect of actin inhibitor treatment on cytoneme extension
(A) Treatment with the cdc42 inhibitor (ML141) significantly reduced cytoneme extension frequency (*P*<0.0001, N=3 larvae per group). Statistical significance was assessed using Student t test. Error bars indicate mean ± SEM.

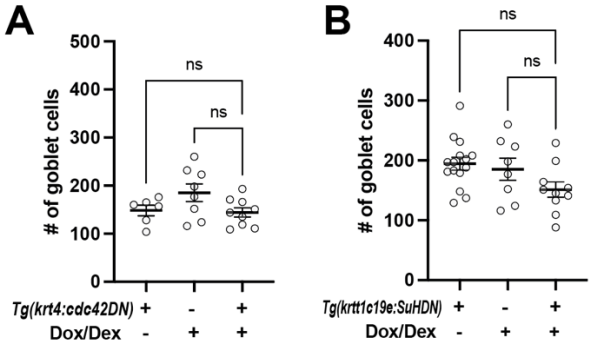

Figure S2. Goblet cell count in the zebrafish epidermis
(A) Quantification of goblet cell numbers revealed no significant difference between two controls and experimental *Tg(krt4:TetGBDTRE-v2a-cdc42DN)* zebrafish ($F_{2,20}$ = 2.763, P = 0.0872, N=23 larvae total).
(B) Quantification of goblet cell numbers showed no significant difference between two controls and experimental *Tg(krtt1c19e:TetGBDTRE-v2a-SuHDN)* zebrafish ($F_{2, 30}$ = 3.040, P = 0.0628, N= 33 larvae total). Statistical significances were assessed by One-way ANOVA followed by Tukey's HSD post hoc test.

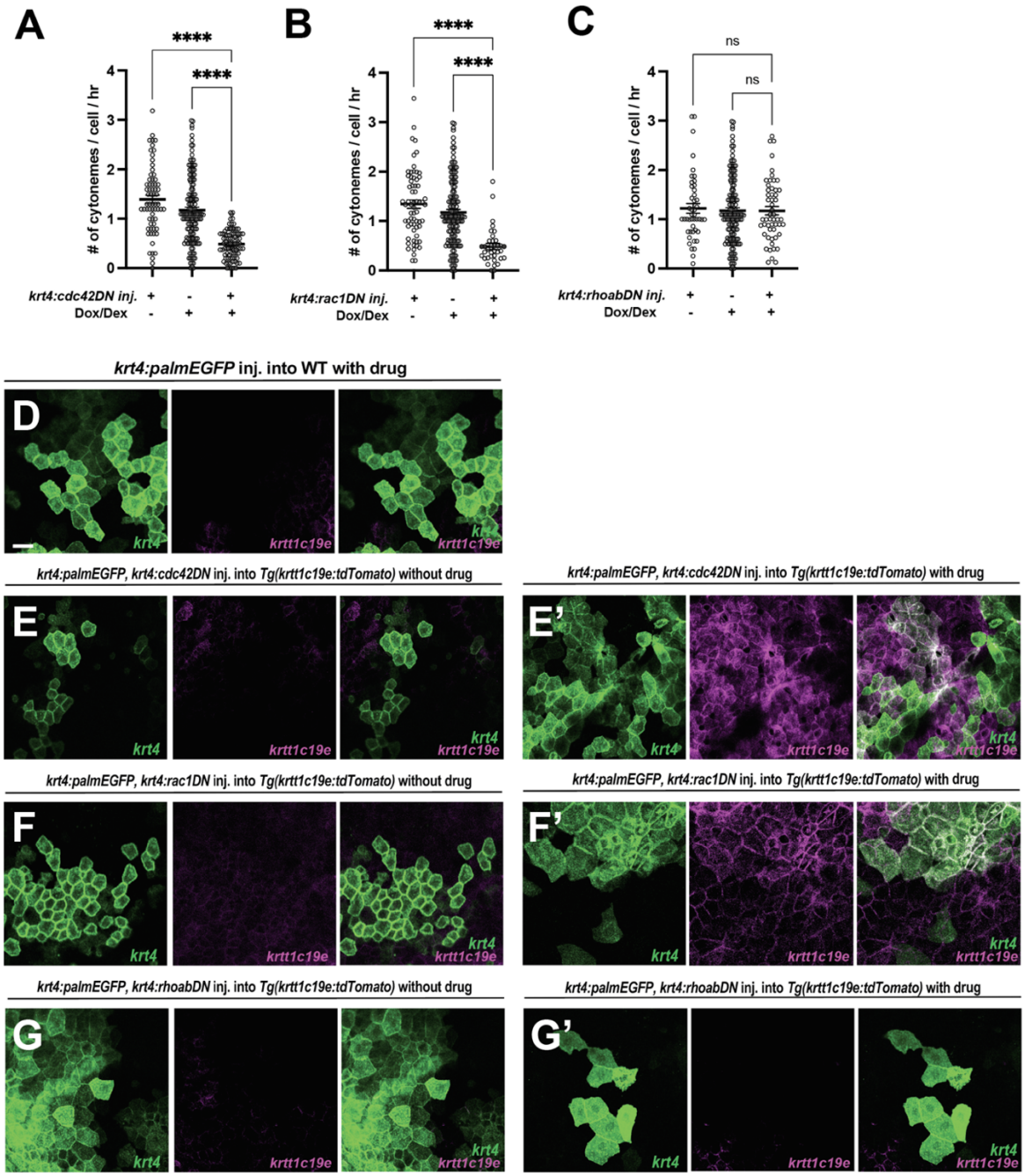

Figure S3. Local manipulations with dominant-negative cdc42, rac1, or rhoab in peridermal keratinocytes

(A) Mosaic expression of *krt4:TetGBDTRE-cdc42DN* in *krt4+* keratinocytes results in a significant reduction in cytoneme extension ($F_{2, 289}$=50.82, P<0.0001, N=292 cells, 9 larvae total), and (E-E') leads to local peridermal disorganization and elevated *krtt1c19e* expression in *krt4+* keratinocytes compared to controls shown in D and E. (B, F-F') Similar phenotypes are observed in *krt4:TetGBDTRE-rac1DN* expressing peridermal keratinocytes as in *krt4:TetGBDTRE-cdc42DN* expressing keratinocytes ($F2_{,239}$=21.43, P<0.0001, N=242 cells, 9 larvae total). (C, G-G') However, local expression of *krt4:TetGBDTRE-rhoabDN* show no effects on cytoneme extension frequency and peridermal keratinocytes ($F_{2,237}$=0.08942, P=0.9145, N=240 cells, 9 larvae total). Statistical significances were assessed by One-way ANOVA followed by Tukey's HSD post hoc test. Scale bars: 20μm. Error bars indicate mean ± SEM.

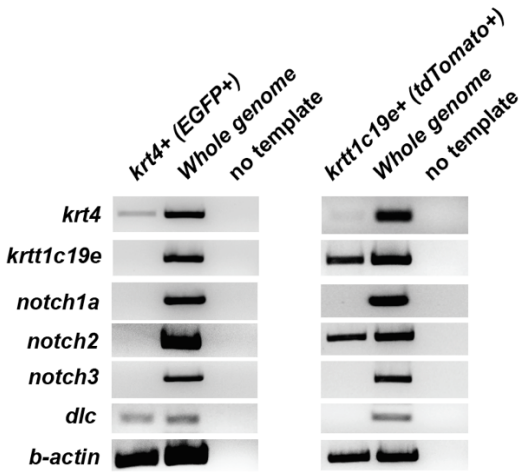

Figure S4. Gene expressions in keratinocytes
RT-PCR analysis revealed the endogenous expression of *krt4, krtt1c19e, notch1a, notch 2, notch 3, and dlc* in keratinocytes. These cells were FACS-sorted for EGFP+ cells from *Tg(krt4:lyn-EGFP)* and for tdTomato+ cells from *Tg(krtt1c19e:tdTomato).* Whole genome cDNA was used as a positive control, and reactions without a template served as negative controls.

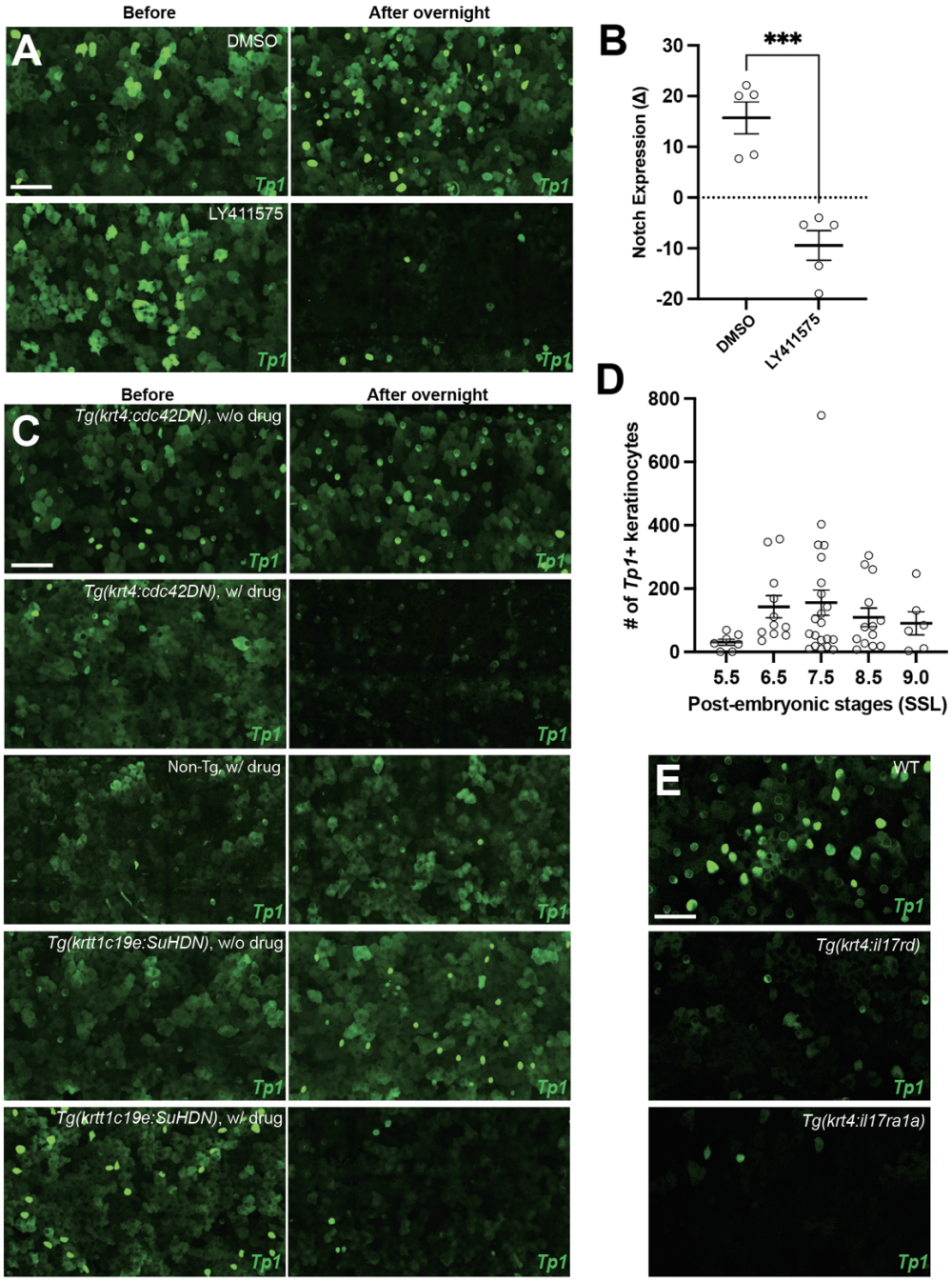

Figure S5. Notch reporter (*Tp1)* expression

(A) Images before and after treatment with DMSO and LY411575 (Notch inhibitor) in the *Tg(Tp1:EGFP)*. (B) Treatment with LY411575 resulted in a significant overall reduction in Notch expression levels in the TP1 Notch reporter line compared to the DMSO control group ($P<0.001$, N=5 larvae per group). (C) Images before and after cytoneme inhibition through drug induction of cdc42DN-expression in *krt4+* keratinocytes and direct inhibition of Notch signaling via drug induction of SuHDN expression in *krtt1c19e+* keratinocytes, along with DMSO treatment. (D) The number of *Tp1+* keratinocytes peaked during epidermal remodeling (SSL6.5-7.5, N=58 larvae total) in zebrafish. (E) A significantly lower number of *Tp1+* keratinocytes were observed in *Tg(krt4:il17rd)* or *Tg(krt4:il17r1a1)* compared to control (Figure 5C). Statistical significance was assessed by Student t test. Scale bars: 100μm (A, C, E). Error bars indicate mean ± SEM.

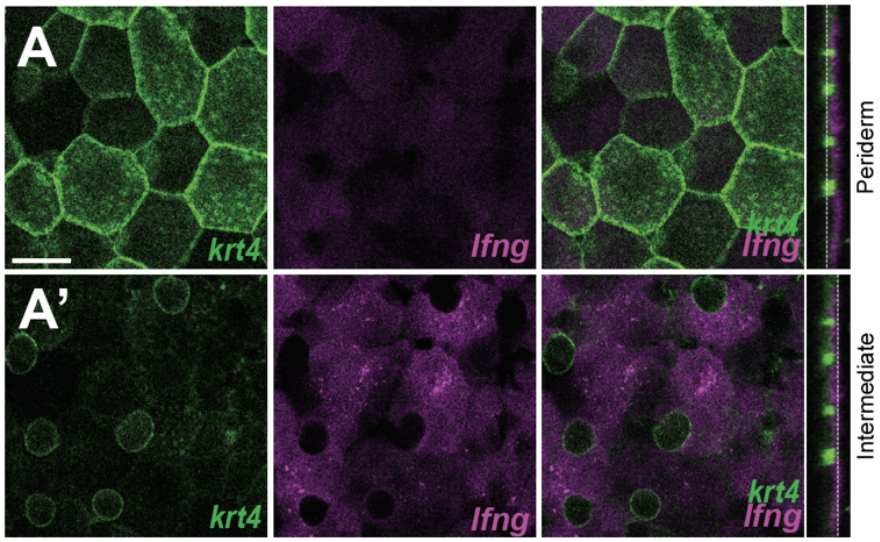

Figure S6. Notch signal modifiers in undifferentiated keratinocytes
(A-A') Images showing *lunatic fringe (lfng)* expression in the intermediate layer of epidermis. Scale bars: 20μm (A-A').

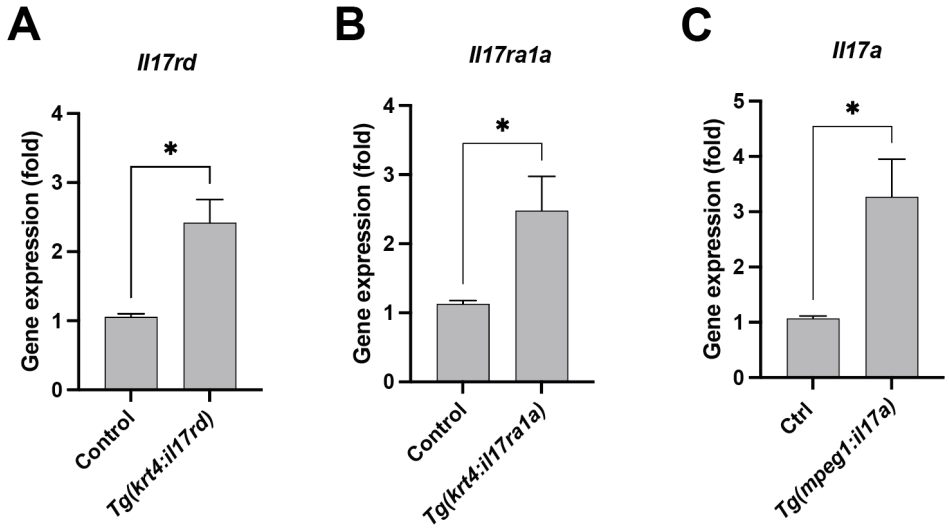

Figure S7. Overexpression *il17rd*, *il17ra1a* or *il17a* in transgenic animals
(A) Quantitative PCR reveals that *il17rd* mRNA is overexpressed in *Tg(krt4:il17rd)* (P=0.0159, N=3 independent experiments). (B) Quantitative PCR shows *il17ra1a* mRNA is overexpressed in *Tg(krt4:il17ra1a)* (P=0.0351, N=4 independent experiments). (C) Quantitative PCR demonstrates that *il17a* mRNA is overexpressed in the skin of *Tg(mpeg1:il17a)* animals (P=0.0183, N=4 independent experiments). Statistical significances were assessed by Student t test. Error bars indicate mean ± SEM.

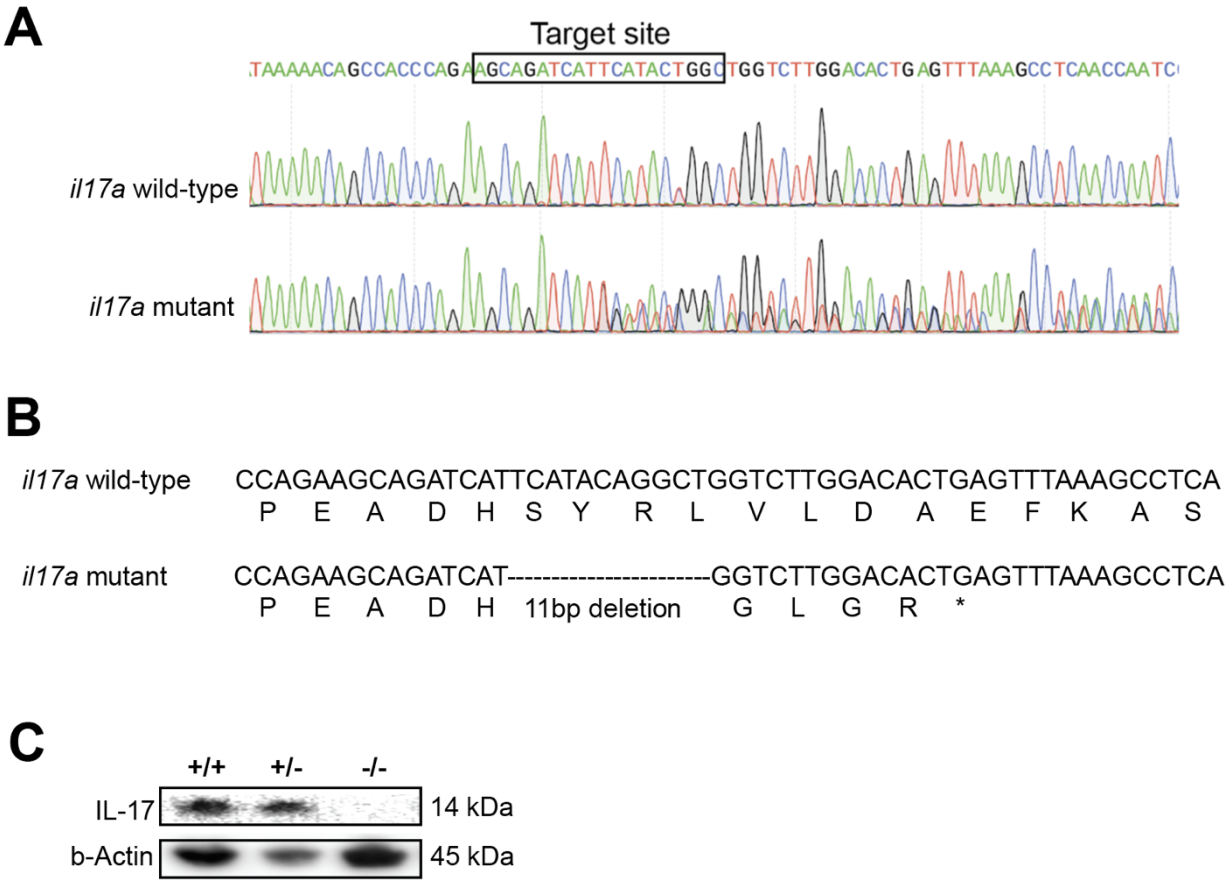

Figure S8. CRISPR/Cas9 induced knockout of zebrafish *il17a* resulting in a premature stop codon

(A) Comparison of Sanger sequencing chromatograms between wild-type and heterozygous *il17a* mutant zebrafish. The region targeted by the single guide RNA is highlighted within the black box. (B) Sanger sequencing of the *il17a* mutant reveals an 11bp deletion, leading to the induction of a premature stop codon. (C) Western blotting confirmed that IL-17 protein expression was not detected in the homozygous *il17a* CRISPR mutants.

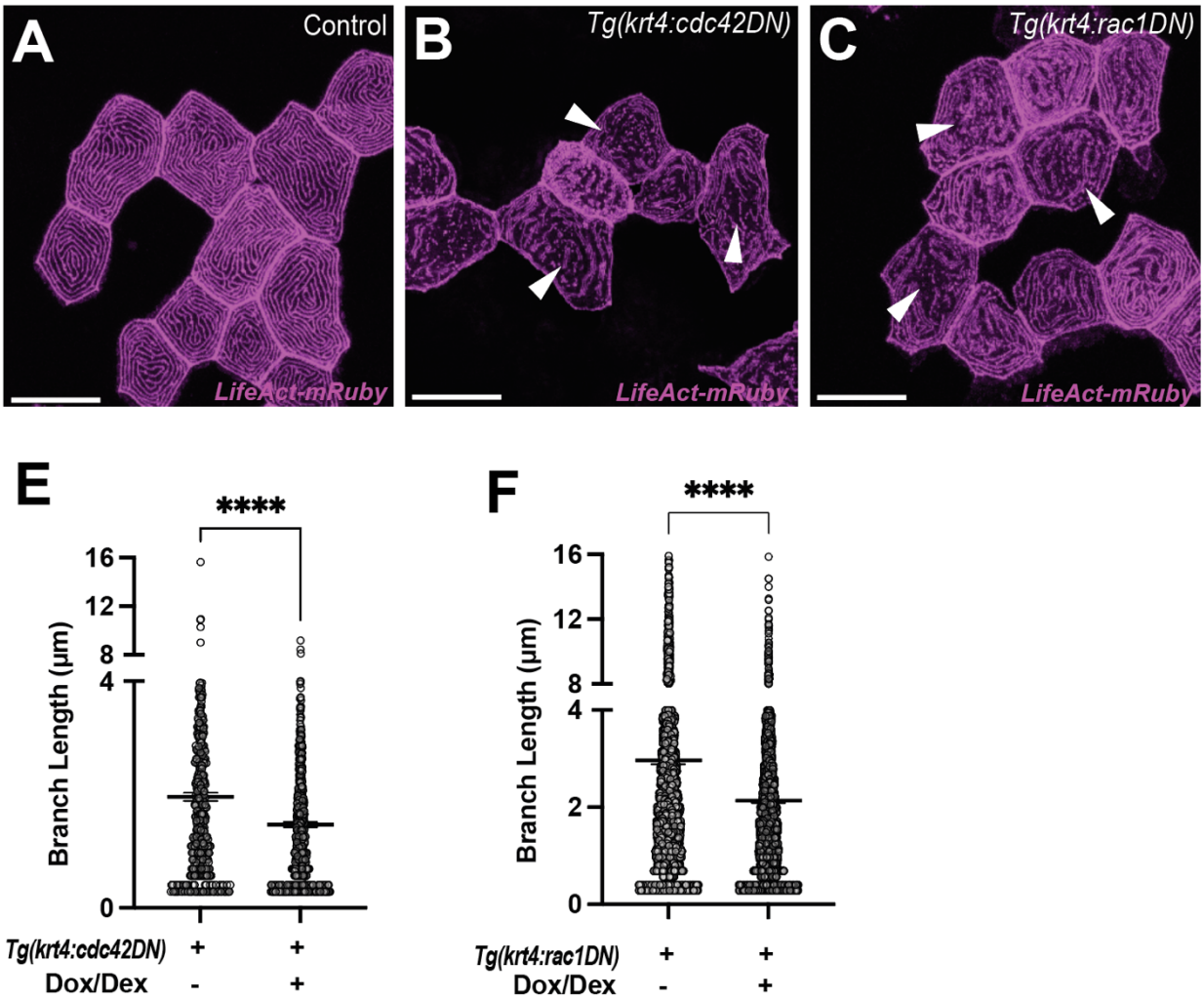

Figure S9. Microridge disorganization in *cdc42DN* or *rac1DN* overexpressed keratinocytes
(A-C) Arrowheads indicate disrupted microridges in *cdc42DN* or *rac1DN* overexpressed keratinocytes. Differentiated keratinocytes (*krt4+*) are mosaicly labeled in the *Tg(krt4:TetGBDTRE-nVenus-cdc42DN)* or *Tg(krt4:TetGBDTRE-nVenus-rac1DN).* These transgenes were induced by administering Dox and Dex. (E) Significantly reduced branch lengths of microrides in the *cdc42DN* (P<0.0001, N=40 cells, 7 larvae total) or (F) *rac1DN* overexpressed cells (P<0.0001, N=66 cells, 6 larvae total). Statistical significances were assessed by Student t test. Scale bars: 20µm (A, B, C). Error bars indicate mean ± SEM.

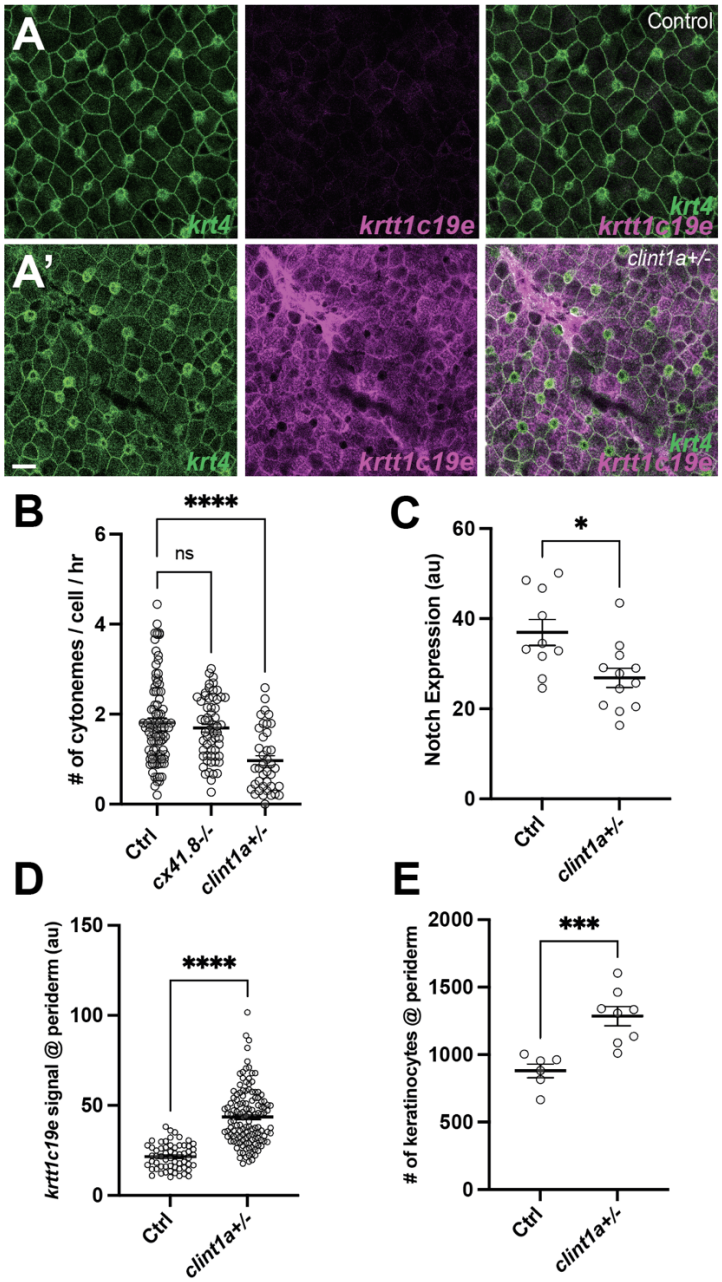

Figure S10. *clint1* regulates epidermal maintenance via keratinocyte cytonemes
(A-A') *clint1* mutants exhibit a disorganized periderm. (B-E) *clint1* mutants show (B) a lower frequency of cytoneme extension as compared to controls (WT, *cx41.8*$^{-/-}$) ($F_{2, 186}$ = 14.55, P<0.0001, N=10 larvae total), (C) reduced Notch responsiveness (P=0.0119, N=12 mutants, N=10 controls), (D) increased *krtt1c19e* expression in the periderm (P<0.0001, N=13 mutants, N=6 controls), and (E) a greater number of keratinocytes within the periderm (P<0.001, N=8 mutants, N=6 controls). Statistical significances were assessed by One-way ANOVA followed by Tukey's HSD post hoc test and Student t test. Scale bars, 20μm (A-A'). Error bars indicate mean ± SEM.

References

1. Akat, E., Yenmis, M., Pombal, M.A., Molist, P., Megias, M., Arman, S., Vesely, M., Anderson, R., and Ayaz, D. (2022). Comparison of vertebrate skin structure at class level: A review. Anat Rec (Hoboken) *305*, 3543-3608. 10.1002/ar.24908.
2. Chang, W.J., and Hwang, P.P. (2011). Development of zebrafish epidermis. Birth Defects Res C Embryo Today *93*, 205-214. 10.1002/bdrc.20215.
3. Segre, J.A. (2006). Epidermal barrier formation and recovery in skin disorders. J Clin Invest *116*, 1150-1158. 10.1172/JCI28521.
4. Lee, R.T., Asharani, P.V., and Carney, T.J. (2014). Basal keratinocytes contribute to all strata of the adult zebrafish epidermis. PLoS One *9*, e84858. 10.1371/journal.pone.0084858.
5. Blanpain, C., and Fuchs, E. (2009). Epidermal homeostasis: a balancing act of stem cells in the skin. Nat Rev Mol Cell Biol *10*, 207-217. 10.1038/nrm2636.
6. Lowes, M.A., Suarez-Farinas, M., and Krueger, J.G. (2014). Immunology of psoriasis. Annu Rev Immunol *32*, 227-255. 10.1146/annurev-immunol-032713-120225.
7. Nowell, C., and Radtke, F. (2013). Cutaneous Notch signaling in health and disease. Cold Spring Harb Perspect Med *3*, a017772. 10.1101/cshperspect.a017772.
8. Schempp, C., Emde, M., and Wolfle, U. (2009). Dermatology in the Darwin anniversary. Part 1: Evolution of the integument. J Dtsch Dermatol Ges *7*, 750-757. 10.1111/j.1610-0387.2009.07193.x.
9. Zhou, X., Chen, Y., Cui, L., Shi, Y., and Guo, C. (2022). Advances in the pathogenesis of psoriasis: from keratinocyte perspective. Cell Death Dis *13*, 81. 10.1038/s41419-022-04523-3.
10. Park, S., Matte-Martone, C., Gonzalez, D.G., Lathrop, E.A., May, D.P., Pineda, C.M., Moore, J.L., Boucher, J.D., Marsh, E., Schmitter-Sanchez, A., et al. (2021). Skin-resident immune cells actively coordinate their distribution with epidermal cells during homeostasis. Nat Cell Biol *23*, 476-484. 10.1038/s41556-021-00670-5.
11. Blanpain, C., Lowry, W.E., Pasolli, H.A., and Fuchs, E. (2006). Canonical notch signaling functions as a commitment switch in the epidermal lineage. Genes Dev *20*, 3022-3035. 10.1101/gad.1477606.
12. Nickoloff, B.J., Qin, J.Z., Chaturvedi, V., Denning, M.F., Bonish, B., and Miele, L. (2002). Jagged-1 mediated activation of notch signaling induces complete maturation of human keratinocytes through NF-kappaB and PPARgamma. Cell Death Differ *9*, 842-855. 10.1038/sj.cdd.4401036.
13. Thelu, J., Rossio, P., and Favier, B. (2002). Notch signalling is linked to epidermal cell differentiation level in basal cell carcinoma, psoriasis and wound healing. BMC Dermatol *2*, 7. 10.1186/1471-5945-2-7.
14. Gratton, R., Tricarico, P.M., Moltrasio, C., Lima Estevao de Oliveira, A.S., Brandao, L., Marzano, A.V., Zupin, L., and Crovella, S. (2020). Pleiotropic Role of Notch Signaling in Human Skin Diseases. Int J Mol Sci *21*. 10.3390/ijms21124214.

15. Ota, T., Takekoshi, S., Takagi, T., Kitatani, K., Toriumi, K., Kojima, T., Kato, M., Ikoma, N., Mabuchi, T., and Ozawa, A. (2014). Notch signaling may be involved in the abnormal differentiation of epidermal keratinocytes in psoriasis. Acta Histochem Cytochem *47*, 175-183. 10.1267/ahc.14027.
16. Rangarajan, A., Talora, C., Okuyama, R., Nicolas, M., Mammucari, C., Oh, H., Aster, J.C., Krishna, S., Metzger, D., Chambon, P., et al. (2001). Notch signaling is a direct determinant of keratinocyte growth arrest and entry into differentiation. EMBO J *20*, 3427-3436. 10.1093/emboj/20.13.3427.
17. Mosca, M., Hong, J., Hadeler, E., Hakimi, M., Liao, W., and Bhutani, T. (2021). The Role of IL-17 Cytokines in Psoriasis. Immunotargets Ther *10*, 409-418. 10.2147/ITT.S240891.
18. Campa, M., Mansouri, B., Warren, R., and Menter, A. (2016). A Review of Biologic Therapies Targeting IL-23 and IL-17 for Use in Moderate-to-Severe Plaque Psoriasis. Dermatol Ther (Heidelb) *6*, 1-12. 10.1007/s13555-015-0092-3.
19. Fragoulis, G.E., Siebert, S., and McInnes, I.B. (2016). Therapeutic Targeting of IL-17 and IL-23 Cytokines in Immune-Mediated Diseases. Annu Rev Med *67*, 337-353. 10.1146/annurev-med-051914-021944.
20. Eom, D.S. (2020). Airinemes: thin cellular protrusions mediate long-distance signalling guided by macrophages. Open Biol *10*, 200039. 10.1098/rsob.200039.
21. Kornberg, T.B., and Roy, S. (2014). Cytonemes as specialized signaling filopodia. Development *141*, 729-736. 10.1242/dev.086223.
22. Ma, L., Li, Y., Peng, J., Wu, D., Zhao, X., Cui, Y., Chen, L., Yan, X., Du, Y., and Yu, L. (2015). Discovery of the migrasome, an organelle mediating release of cytoplasmic contents during cell migration. Cell Res *25*, 24-38. 10.1038/cr.2014.135.
23. Melentijevic, I., Toth, M.L., Arnold, M.L., Guasp, R.J., Harinath, G., Nguyen, K.C., Taub, D., Parker, J.A., Neri, C., Gabel, C.V., et al. (2017). C. elegans neurons jettison protein aggregates and mitochondria under neurotoxic stress. Nature *542*, 367-371. 10.1038/nature21362.
24. Zhang, C., and Scholpp, S. (2019). Cytonemes in development. Curr Opin Genet Dev *57*, 25-30. 10.1016/j.gde.2019.06.005.
25. Daly, C.A., Hall, E.T., and Ogden, S.K. (2022). Regulatory mechanisms of cytoneme-based morphogen transport. Cell Mol Life Sci *79*, 119. 10.1007/s00018-022-04148-x.
26. Hall, E.T., Dillard, M.E., Cleverdon, E.R., Zhang, Y., Daly, C.A., Ansari, S.S., Wakefield, R., Stewart, D.P., Pruett-Miller, S.M., Lavado, A., et al. (2023). Cytoneme signaling provides essential contributions to mammalian tissue patterning. Cell. 10.1016/j.cell.2023.12.003.
27. Kornberg, T.B., and Roy, S. (2014). Communicating by touch--neurons are not alone. Trends Cell Biol *24*, 370-376. 10.1016/j.tcb.2014.01.003.
28. Eisenhoffer, G.T., Slattum, G., Ruiz, O.E., Otsuna, H., Bryan, C.D., Lopez, J., Wagner, D.S., Bonkowsky, J.L., Chien, C.B., Dorsky, R.I., and Rosenblatt, J. (2017). A toolbox to study epidermal cell types in zebrafish. J Cell Sci *130*, 269-277. 10.1242/jcs.184341.

29. Li, Q., Frank, M., Thisse, C.I., Thisse, B.V., and Uitto, J. (2011). Zebrafish: a model system to study heritable skin diseases. J Invest Dermatol *131*, 565-571. 10.1038/jid.2010.388.
30. Martinez-Navarro, F.J., Martinez-Menchon, T., Mulero, V., and Galindo-Villegas, J. (2019). Models of human psoriasis: Zebrafish the newly appointed player. Dev Comp Immunol *97*, 76-87. 10.1016/j.dci.2019.03.018.
31. Dodd, M.E., Hatzold, J., Mathias, J.R., Walters, K.B., Bennin, D.A., Rhodes, J., Kanki, J.P., Look, A.T., Hammerschmidt, M., and Huttenlocher, A. (2009). The ENTH domain protein Clint1 is required for epidermal homeostasis in zebrafish. Development *136*, 2591-2600. 10.1242/dev.038448.
32. Sahlen, P., Spalinskas, R., Asad, S., Mahapatra, K.D., Hojer, P., Anil, A., Eisfeldt, J., Srivastava, A., Nikamo, P., Mukherjee, A., et al. (2021). Chromatin interactions in differentiating keratinocytes reveal novel atopic dermatitis- and psoriasis-associated genes. J Allergy Clin Immunol *147*, 1742-1752. 10.1016/j.jaci.2020.09.035.
33. Bowman, R.L., Wang, D., and Eom, D.S. (2023). A macrophage subpopulation promotes airineme-mediated intercellular communication in a matrix metalloproteinase-9 dependent manner. Cell Rep *42*, 112818. 10.1016/j.celrep.2023.112818.
34. Eom, D.S., Bain, E.J., Patterson, L.B., Grout, M.E., and Parichy, D.M. (2015). Long-distance communication by specialized cellular projections during pigment pattern development and evolution. Elife *4*. 10.7554/eLife.12401.
35. Eom, D.S., and Parichy, D.M. (2017). A macrophage relay for long-distance signaling during postembryonic tissue remodeling. Science *355*, 1317-1320. 10.1126/science.aal2745.
36. Park, S., Kim, H., Wang, Y., Eom, D.S., and Allard, J. (2022). Zebrafish airinemes optimize their shape between ballistic and diffusive search. Elife *11*. 10.7554/eLife.75690.
37. Parichy, D.M., Elizondo, M.R., Mills, M.G., Gordon, T.N., and Engeszer, R.E. (2009). Normal table of postembryonic zebrafish development: staging by externally visible anatomy of the living fish. Dev Dyn *238*, 2975-3015. 10.1002/dvdy.22113.
38. Knopf, F., Schnabel, K., Haase, C., Pfeifer, K., Anastassiadis, K., and Weidinger, G. (2010). Dually inducible TetON systems for tissue-specific conditional gene expression in zebrafish. Proc Natl Acad Sci U S A *107*, 19933-19938. 10.1073/pnas.1007799107.
39. Moriyama, M., Durham, A.D., Moriyama, H., Hasegawa, K., Nishikawa, S., Radtke, F., and Osawa, M. (2008). Multiple roles of Notch signaling in the regulation of epidermal development. Dev Cell *14*, 594-604. 10.1016/j.devcel.2008.01.017.
40. Nguyen, B.C., Lefort, K., Mandinova, A., Antonini, D., Devgan, V., Della Gatta, G., Koster, M.I., Zhang, Z., Wang, J., Tommasi di Vignano, A., et al. (2006). Cross-regulation between Notch and p63 in keratinocyte commitment to differentiation. Genes Dev *20*, 1028-1042. 10.1101/gad.1406006.
41. Parsons, M.J., Pisharath, H., Yusuff, S., Moore, J.C., Siekmann, A.F., Lawson, N., and Leach, S.D. (2009). Notch-responsive cells initiate the secondary

transition in larval zebrafish pancreas. Mech Dev *126*, 898-912. 10.1016/j.mod.2009.07.002.
42. Liu, J., Sun, Y.H., Wang, N., Wang, Y.P., and Zhu, Z.Y. (2006). Cloning, characterization and promoter analysis of common carp hairy/Enhancer-of-split-related gene, her6. J Genet *85*, 171-178. 10.1007/BF02935327.
43. Dale, J.K., Maroto, M., Dequeant, M.L., Malapert, P., McGrew, M., and Pourquie, O. (2003). Periodic notch inhibition by lunatic fringe underlies the chick segmentation clock. Nature *421*, 275-278. 10.1038/nature01244.
44. Panin, V.M., Papayannopoulos, V., Wilson, R., and Irvine, K.D. (1997). Fringe modulates Notch-ligand interactions. Nature *387*, 908-912. 10.1038/43191.
45. Abdou, A.G., Maraee, A.H., Sharaf, A., and Elnaidany, N.F. (2012). Up-regulation of Notch-1 in psoriasis: an immunohistochemical study. Ann Diagn Pathol *16*, 177-184. 10.1016/j.anndiagpath.2011.09.005.
46. Armstrong, A.W., and Read, C. (2020). Pathophysiology, Clinical Presentation, and Treatment of Psoriasis: A Review. JAMA *323*, 1945-1960. 10.1001/jama.2020.4006.
47. Gonzalez-Fernandez, C., Chaves-Pozo, E., and Cuesta, A. (2020). Identification and Regulation of Interleukin-17 (IL-17) Family Ligands in the Teleost Fish European Sea Bass. Int J Mol Sci *21*. 10.3390/ijms21072439.
48. Wu, B., Jin, M., Zhang, Y., Wei, T., and Bai, Z. (2011). Evolution of the IL17 receptor family in chordates: a new subfamily IL17REL. Immunogenetics *63*, 835-845. 10.1007/s00251-011-0554-4.
49. Borowczyk, J., Buerger, C., Tadjrischi, N., Drukala, J., Wolnicki, M., Wnuk, D., Modarressi, A., Boehncke, W.H., and Brembilla, N.C. (2020). IL-17E (IL-25) and IL-17A Differentially Affect the Functions of Human Keratinocytes. J Invest Dermatol *140*, 1379-1389 e1372. 10.1016/j.jid.2019.12.013.
50. Das, S., Srinivasan, S., Srivastava, A., Kumar, S., Das, G., Das, S., Dwivedi, A., Karulkar, A., Makkad, K., Bilala, R., et al. (2019). Differential Influence of IL-9 and IL-17 on Actin Cytoskeleton Regulates the Migration Potential of Human Keratinocytes. J Immunol *202*, 1949-1961. 10.4049/jimmunol.1800823.
51. Pinto, C.S., Khandekar, A., Bhavna, R., Kiesel, P., Pigino, G., and Sonawane, M. (2019). Microridges are apical epithelial projections formed of F-actin networks that organize the glycan layer. Sci Rep *9*, 12191. 10.1038/s41598-019-48400-0.
52. van Loon, A.P., Erofeev, I.S., Maryshev, I.V., Goryachev, A.B., and Sagasti, A. (2020). Cortical contraction drives the 3D patterning of epithelial cell surfaces. J Cell Biol *219*. 10.1083/jcb.201904144.
53. Hall, A. (1998). Rho GTPases and the actin cytoskeleton. Science *279*, 509-514. 10.1126/science.279.5350.509.
54. Jaffe, A.B., and Hall, A. (2005). Rho GTPases: biochemistry and biology. Annu Rev Cell Dev Biol *21*, 247-269. 10.1146/annurev.cellbio.21.020604.150721.
55. Stanganello, E., Hagemann, A.I., Mattes, B., Sinner, C., Meyen, D., Weber, S., Schug, A., Raz, E., and Scholpp, S. (2015). Filopodia-based Wnt transport during vertebrate tissue patterning. Nat Commun *6*, 5846. 10.1038/ncomms6846.
56. Wasiak, S., Legendre-Guillemin, V., Puertollano, R., Blondeau, F., Girard, M., de Heuvel, E., Boismenu, D., Bell, A.W., Bonifacino, J.S., and McPherson, P.S.

(2002). Enthoprotin: a novel clathrin-associated protein identified through subcellular proteomics. J Cell Biol *158*, 855-862. 10.1083/jcb.200205078.
57. Roy, S., Hsiung, F., and Kornberg, T.B. (2011). Specificity of Drosophila cytonemes for distinct signaling pathways. Science *332*, 354-358. 10.1126/science.1198949.
58. Thelu, J., Viallet, J.P., and Dhouailly, D. (1998). Differential expression pattern of the three Fringe genes is associated with epidermal differentiation. J Invest Dermatol *111*, 903-906. 10.1046/j.1523-1747.1998.00372.x.
59. Liu, T., Li, S., Ying, S., Tang, S., Ding, Y., Li, Y., Qiao, J., and Fang, H. (2020). The IL-23/IL-17 Pathway in Inflammatory Skin Diseases: From Bench to Bedside. Front Immunol *11*, 594735. 10.3389/fimmu.2020.594735.
60. Blauvelt, A., and Chiricozzi, A. (2018). The Immunologic Role of IL-17 in Psoriasis and Psoriatic Arthritis Pathogenesis. Clin Rev Allergy Immunol *55*, 379-390. 10.1007/s12016-018-8702-3.
61. Pasparakis, M., Courtois, G., Hafner, M., Schmidt-Supprian, M., Nenci, A., Toksoy, A., Krampert, M., Goebeler, M., Gillitzer, R., Israel, A., et al. (2002). TNF-mediated inflammatory skin disease in mice with epidermis-specific deletion of IKK2. Nature *417*, 861-866. 10.1038/nature00820.
62. Zenz, R., Eferl, R., Kenner, L., Florin, L., Hummerich, L., Mehic, D., Scheuch, H., Angel, P., Tschachler, E., and Wagner, E.F. (2005). Psoriasis-like skin disease and arthritis caused by inducible epidermal deletion of Jun proteins. Nature *437*, 369-375. 10.1038/nature03963.
63. Dubin-Bar, D., Bitan, A., Bakhrat, A., Kaiden-Hasson, R., Etzion, S., Shaanan, B., and Abdu, U. (2008). The Drosophila IKK-related kinase (Ik2) and Spindle-F proteins are part of a complex that regulates cytoskeleton organization during oogenesis. BMC Cell Biol *9*, 51. 10.1186/1471-2121-9-51.
64. Lennikov, A., Mirabelli, P., Mukwaya, A., Schaupper, M., Thangavelu, M., Lachota, M., Ali, Z., Jensen, L., and Lagali, N. (2018). Selective IKK2 inhibitor IMD0354 disrupts NF-kappaB signaling to suppress corneal inflammation and angiogenesis. Angiogenesis *21*, 267-285. 10.1007/s10456-018-9594-9.
65. Otani, T., Ogura, Y., Misaki, K., Maeda, T., Kimpara, A., Yonemura, S., and Hayashi, S. (2016). IKKepsilon inhibits PKC to promote Fascin-dependent actin bundling. Development *143*, 3806-3816. 10.1242/dev.138495.
66. Kalthoff, C., Groos, S., Kohl, R., Mahrhold, S., and Ungewickell, E.J. (2002). Clint: a novel clathrin-binding ENTH-domain protein at the Golgi. Mol Biol Cell *13*, 4060-4073. 10.1091/mbc.e02-03-0171.
67. Barros-Becker, F., Lam, P.Y., Fisher, R., and Huttenlocher, A. (2017). Live imaging reveals distinct modes of neutrophil and macrophage migration within interstitial tissues. J Cell Sci *130*, 3801-3808. 10.1242/jcs.206128.
68. Friedman, J.R., Webster, B.M., Mastronarde, D.N., Verhey, K.J., and Voeltz, G.K. (2010). ER sliding dynamics and ER-mitochondrial contacts occur on acetylated microtubules. J Cell Biol *190*, 363-375. 10.1083/jcb.200911024.
69. Xue, J., and Corti, P. (2022). Stain-Free Approach for Western Blot Analysis of Zebrafish Embryos. Methods Mol Biol *2498*, 387-396. 10.1007/978-1-0716-2313-8_23.